SJSU SAN JOSÉ STATE UNIVERSITY

MTI MINETA TRANSPORTATION INSTITUTE

Roadside Asset Extraction from Mobile LiDAR Point Cloud

Yushin Ahn, PhD Riadh Munjy, PhD Stephen Choi, PhD

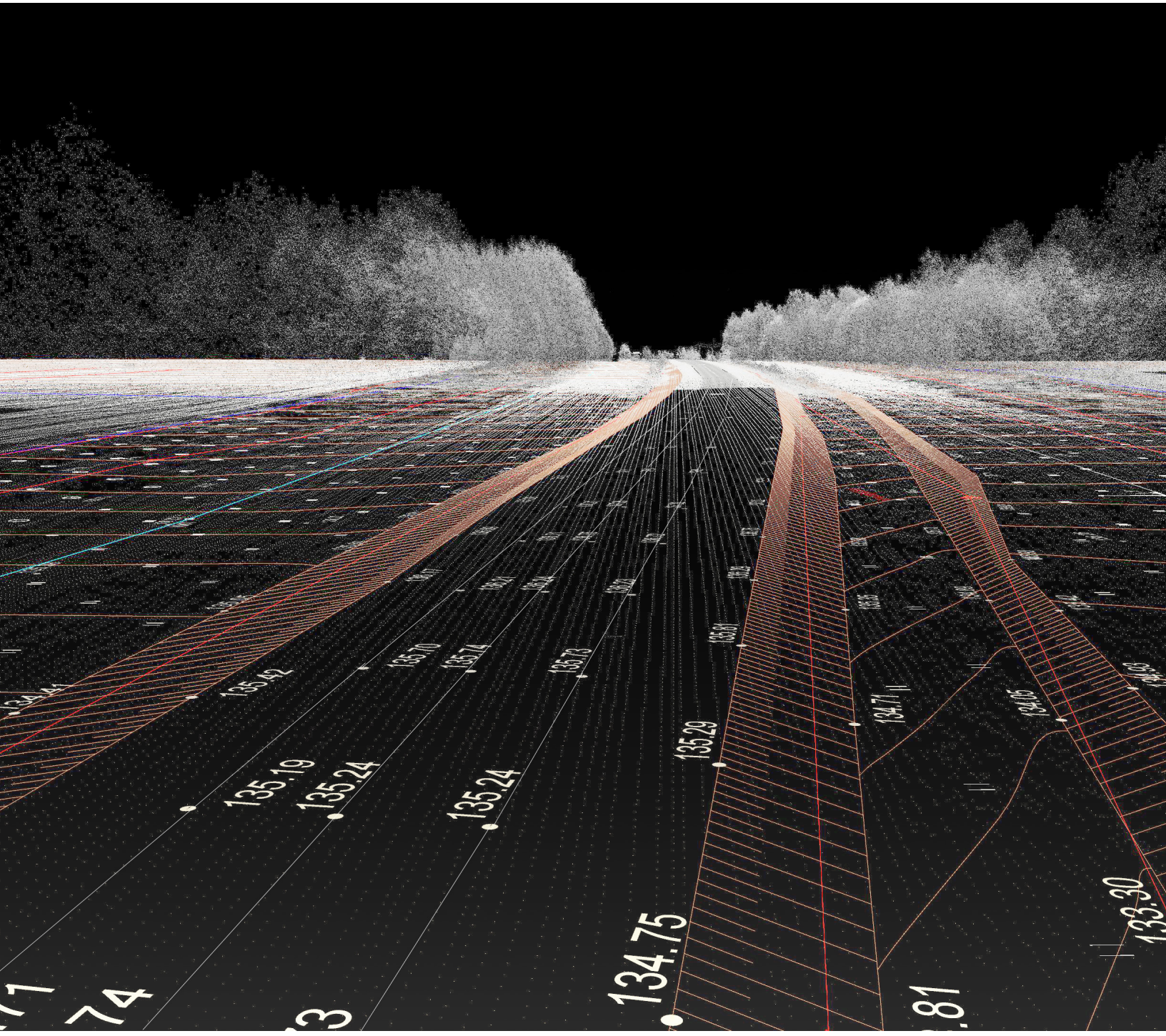

CSUTC California State University Transportation Consortium

FRESNO STATE Discovery. Diversity. Distinction.

CSU TRANSPORTATION CONSORTIUM transweb.sjsu.edu/csutc

MINETA TRANSPORTATION INSTITUTE

Founded in 1991, the Mineta Transportation Institute (MTI), an organized research and training unit in partnership with the Lucas College and Graduate School of Business at San José State University (SJSU), increases mobility for all by improving the safety, efficiency, accessibility, and convenience of our nation's transportation system. Through research, education, workforce development, and technology transfer, we help create a connected world. MTI leads the California State University Transportation Consortium (CSUTC) funded by the State of California through Senate Bill 1 and the Climate Change and Extreme Events Training and Research (CCEETR) Program funded by the Federal Railroad Administration. MTI focuses on three primary responsibilities:

Research

MTI conducts multi-disciplinary research focused on surface transportation that contributes to effective decision making. Research areas include: active transportation; planning and policy; security and counterterrorism; sustainable transportation and land use; transit and passenger rail; transportation engineering; transportation finance; transportation technology; and workforce and labor. MTI research publications undergo expert peer review to ensure the quality of the research.

Education and Workforce Development

To ensure the efficient movement of people and goods, we must prepare the next generation of skilled transportation professionals who can lead a thriving, forward-thinking transportation industry for a more connected world. To help achieve this, MTI sponsors a suite of workforce development and education opportunities. The Institute supports educational programs offered by the Lucas Graduate School of Business: a Master of Science in Transportation Management, plus graduate certificates that include High-Speed and Intercity Rail Management and Transportation Security Management. These flexible programs offer live online classes so that working transportation professionals can pursue an advanced degree regardless of their location.

Information and Technology Transfer

MTI utilizes a diverse array of dissemination methods and media to ensure research results reach those responsible for managing change. These methods include publication, seminars, workshops, websites, social media, webinars, and other technology transfer mechanisms. Additionally, MTI promotes the availability of completed research to professional organizations and works to integrate the research findings into the graduate education program. MTI's extensive collection of transportation-related publications is integrated into San José State University's world-class Martin Luther King, Jr. Library.

Report 25-15

Roadside Asset Extraction from Mobile LiDAR Point Cloud

Yushin Ahn, PhD

Riadh Munjy, PhD

Stephen Choi, PhD

August 2025

A publication of the
Mineta Transportation Institute
Created by Congress in 1991

College of Business
San José State University
San José, CA 95192-0219

TECHNICAL REPORT DOCUMENTATION PAGE

1. Report No. 25-15	**2. Government Accession No.**	**3. Recipient's Catalog No.**	
4. Title and Subtitle Roadside Asset Extraction from Mobile LiDAR Point Cloud		**5. Report Date** August 2025	
		6. Performing Organization Code	
7. Authors Yushin Ahn, PhD Riadh Munjy, PhD Stephen Choi, PhD		**8. Performing Organization Report** CA-MTI-2448	
9. Performing Organization Name and Address Mineta Transportation Institute College of Business San José State University San José, CA 95192-0219		**10. Work Unit No.**	
		11. Contract or Grant No. SB1-SJAUX_2023-26	
12. Sponsoring Agency Name and Address State of California SB1 2017/2018 Trustees of the California State University Sponsored Programs Administration 401 Golden Shore, 5th Floor Long Beach, CA 90802		**13. Type of Report and Period Covered**	
		14. Sponsoring Agency Code	
15. Supplemental Notes 10.31979/mti.2025.2448			

16. Abstract

Mobile LiDAR systems are powerful tools that help us map roads and their surroundings in 3D with great speed and precision. The data provided by these systems support urban planning efforts, digital mapping, transportation infrastructure maintenance, and more. This report presents a comprehensive workflow for roadside asset extraction using Mobile Terrestrial Laser Scanning (MTLS) data, focusing on road lane detection, cross-section slope analysis, and point cloud classification. Roadside asset extraction is the identification and classification of roadside features like signs and poles. The dataset, acquired using a high-resolution mobile LiDAR system, contains over 5.7 billion points (pieces of data) across 68 LAS files. Preprocessing of the data involved tiling, merging, and denoising processes to enhance data quality. This research used two types of image-like maps—one showing elevation and one showing how reflective the surface is—to model the road and identify lane markings. Furthermore, the team developed and trained an AI-driven deep learning-based classifier program using a PointNet-style architecture implemented in PyTorch to segment ground and non-ground features. The classifier was trained using over 500 million labeled points and applied to new LAS files for inference. The model achieved effective binary classification performance and produced classified LAS outputs compatible with downstream GIS workflows. This means the program was able to successfully sort features into two categories—like ground vs. non-ground—and produce files that work with common mapping software. This work demonstrates the feasibility of combining traditional feature extraction with modern deep learning approaches to enhance automation and accuracy in infrastructure mapping.

17. Key Words Artificial intelligence, laser radar, deep learning, spatial analysis, intelligent transportation systems.	**18. Distribution Statement** No restrictions. This document is available to the public through The National Technical Information Service, Springfield, VA 22161.		
19. Security Classif. (of this report) Unclassified	**20. Security Classif. (of this page)** Unclassified	**21. No. of Pages** 50	**22. Price**

Form DOT F 1700.7 (8-72)

10.31979/mti.2025.2448

Mineta Transportation Institute
College of Business
San José State University
San José, CA 95192-0219

Tel: (408) 924-7560
Fax: (408) 924-7565
Email: mineta-institute@sjsu.edu

transweb.sjsu.edu/research/2448

CONTENTS

List of Figures vii

List of Tables ix

Executive Summary 1

1. Introduction 2

2. Mobile Terrestrial Laser Scanning Data 3

    2.1 MTLS Data Set 3

    2.2 Pre-Processing 4

3. Roadside Assets 7

    3.1 Road Lanes in MTLS Data 7

    3.2 Cross Section Slope Analysis on the Road 15

    3.3 Assessment of Existing LiDAR Point Cloud Processing Programs 25

    3.4 Deep Learning Point Classification Using Python 31

4. Summary and Conclusion 36

Glossary 37

Bibliography 38

About the Authors 40

List of Figures

Figure 1. Trajectory Plot of MTLS Data in Highway 76 4

Figure 2. Illustration of Subset Rectangle Boundaries of LAZ Files 5

Figure 3. Example of Shadow Effect in Laser Scan 5

Figure 4. Ground Points, Non-Ground Points, and Original Point 9

Figure 5. Digital Elevation Model and Intensity Map 12

Figure 6. Black and White Image (upper left), Sobel Edge Image (lower left), and Road Lane Detected (right) 14

Figure 7. Road Lanes Extracted from 3 Tiles of Data (upper) and Google Earth Pro Image of Said Road 15

Figure 8. Illustration of Cross-Section Extraction Scheme. 18

Figure 9. Cross-Section Profile Test 1 19

Figure 10. Cross-Section Profile Test 1, 3D View 20

Figure 11. Cross-Section Profile Test 2 21

Figure 12. Cross-Section Profile Test 3 23

Figure 13. Results of Three Cross-Sections 24

Figure 14. Trimble Business Center Point Cloud Processing Menu 26

Figure 15. Result of Trimble Business Center (TBC) Deep Learning Point Cloud Classification 26

Figure 16. Global Mapper LiDAR Processing Menu 28

Figure 17. Result of Cyclone 3DR Automatic Point Cloud Classification 30

Figure 18. Labeled Data for Deep Learning Point Cloud Classification 33

Figure 19. Python-based Point Cloud Classification Result 35

Figure 20. Point Cloud Classification Result for Tile 14, 15, and 16 35

LIST OF TABLES

Table 1. Cross-section Profile Test 1 Result 20

Table 2. Cross-section Profile Test 2 Result 22

Table 3. Cross-section Profile Test 3 Result 24

Table 4. Comparative Analysis of LiDAR Processing Software 30

Table 5. Labeled Data Statistics 33

Executive Summary

This report outlines a robust pipeline for roadside asset extraction from mobile LiDAR data, integrating traditional processing and deep learning techniques. The MTLS dataset, captured along Highway 76 in Southern California, comprises 5.7 billion points and includes both main and secondary road scans. The workflow begins with efficient data preprocessing, including tiling and denoising to mitigate shadow effects and enhance point density.

Key components of the workflow include road lane extraction through elevation and intensity rasters, and cross-section slope analysis based on Digital Elevation Models (DEM). Lane markings were extracted using adaptive intensity thresholding and edge detection, achieving strong visual alignment with actual road features.

For classification, a deep learning model based on PointNet was trained on over 500 million labeled points to distinguish between ground, vegetation, buildings, poles, and other features. The model demonstrated effective classification performance across different tiles, with clear separation of asset types. Comparison with commercial tools (e.g., TBC, GMP, Cyclone 3DR) revealed that the Python-based approach provides a flexible and automated alternative with competitive accuracy.

This work validates the effectiveness of combining classical GIS methods with deep learning to support asset management, smart city initiatives, and intelligent transportation systems.

1. Introduction

With the advancement of LiDAR (Light Detection and Ranging) technology, point cloud data has become a crucial resource for various applications in transportation, urban planning, and infrastructure management. Mobile LiDAR systems, such as the VMX-1HA, enable the collection of high-density 3D point cloud data, offering unprecedented accuracy and detail in road surface analysis. This report focuses on the processing of LAS point cloud data to extract road lane markings, perform slope analysis, and implement deep learning techniques for automated classification.

Road lane extraction from point cloud data is essential for autonomous navigation, traffic management, and roadway maintenance (Kumar et al., 2013; Chen et al., 2009). By leveraging feature-based and intensity-based filtering techniques, road markings can be detected and delineated efficiently. Slope analysis (Yen et al., 2011), on the other hand, plays a critical role in assessing roadway safety, drainage design, and erosion control. Using elevation and gradient computations, slope variations along road networks can be quantified to support civil engineering and transportation studies, such as pavement design, drainage planning, and the evaluation of erosion risks. Accurate slope profiling helps ensure compliance with design standards and improves stormwater management.

Recent advancements in deep learning have further enhanced the capability to classify point clouds with high precision. Traditional classification methods rely on rule-based segmentation, whereas deep learning approaches, such as PointNet and PointNet++, utilize neural networks to learn complex spatial patterns within the data (Qi et al., 2017). This study integrates deep learning-based classification to distinguish between ground, vegetation, buildings, road surfaces, and other urban features, optimizing the interpretation of LiDAR datasets.

This report provides a comprehensive overview of the methodologies used to process LAS point cloud data, including pre-processing, feature extraction, and classification techniques. The findings contribute to the ongoing efforts in improving the accuracy and automation of LiDAR-based roadway analysis and infrastructure monitoring.

2. Mobile Terrestrial Laser Scanning Data

Mobile Terrestrial Laser Scanning (MTLS) represents a significant advancement in geospatial data acquisition technology. By mounting LiDAR sensors on moving platforms, such as vehicles, MTLS enables the rapid collection of high-density point cloud data across extensive areas. Unlike traditional static methods, MTLS combines the mobility of the collection platform with the precision of laser scanning, facilitating efficient data acquisition in dynamic environments.

Modern MTLS systems integrate multiple technologies, including LiDAR sensors, Global Navigation Satellite Systems (GNSS), Inertial Measurement Units (IMU), and digital imaging devices. This integration ensures accurate georeferencing of collected point clouds, with positioning errors typically below 5cm under optimal conditions. (Lin et al., 2021, Rashdi et al., 2024) The resulting datasets provide unprecedented detail of roadways and surrounding infrastructure, with point densities often exceeding hundreds of points per square meter. As Yen et al. (2011) mentioned, the mobile LiDAR system provides multiple benefits, including safety, efficiency, and comparison with airborne LiDAR and other static LiDAR. This comparison enables cross-validation of data accuracy.

The accuracy of MTLS depends significantly on the proper integration and calibration of positioning components. The fusion of GNSS and IMU data through sophisticated algorithms enables continuous positioning even in areas with poor satellite visibility, such as urban canyons or tunnels.

The processing of MTLS data involves several key steps, including point cloud preprocessing, noise filtering, feature extraction, and classification. Preprocessing ensures the removal of redundant and erroneous points caused by reflections or misalignment. Feature extraction techniques enable the identification of road lanes, sidewalks, slopes, and other urban features. Furthermore, advancements in deep learning-based classification have enhanced the automation and accuracy of point cloud interpretation, distinguishing between ground, vegetation, buildings, poles, and other elements.

The integration of MTLS with geospatial analysis and machine learning techniques has significantly improved the efficiency and accuracy of infrastructure monitoring and roadway analysis. By leveraging high-resolution point cloud data, engineers and researchers can develop more precise models for transportation planning, safety assessments, and automated mapping. As MTLS technology continues to evolve, its applications are expected to broaden, particularly in areas such as infrastructure monitoring, autonomous navigation, and environmental analysis.

2.1 MTLS Data Set

The dataset was collected on Highway 76, between Los Angeles and San Diego, covering approximately 8 miles of roadway. Multiple scans were conducted, including both main lanes and

secondary roads. When accounting for all scan passes and overlapping routes, the total scanning distance amounts to approximately 173 miles.

The dataset contains a total of 68 LAS files: 8 files of main roads and 60 files of arterial roads, with a total file size of 39.4 GB.

- 8 main roads: 440,4701,236 points (4.4 billion)
- 60 secondary roads: 130,4700,884 points (1.3 billion)
- Total number of points: 5,709402,120 points (5.7 billion)

Figure 1. Trajectory Plot of MTLS Data in Highway 76

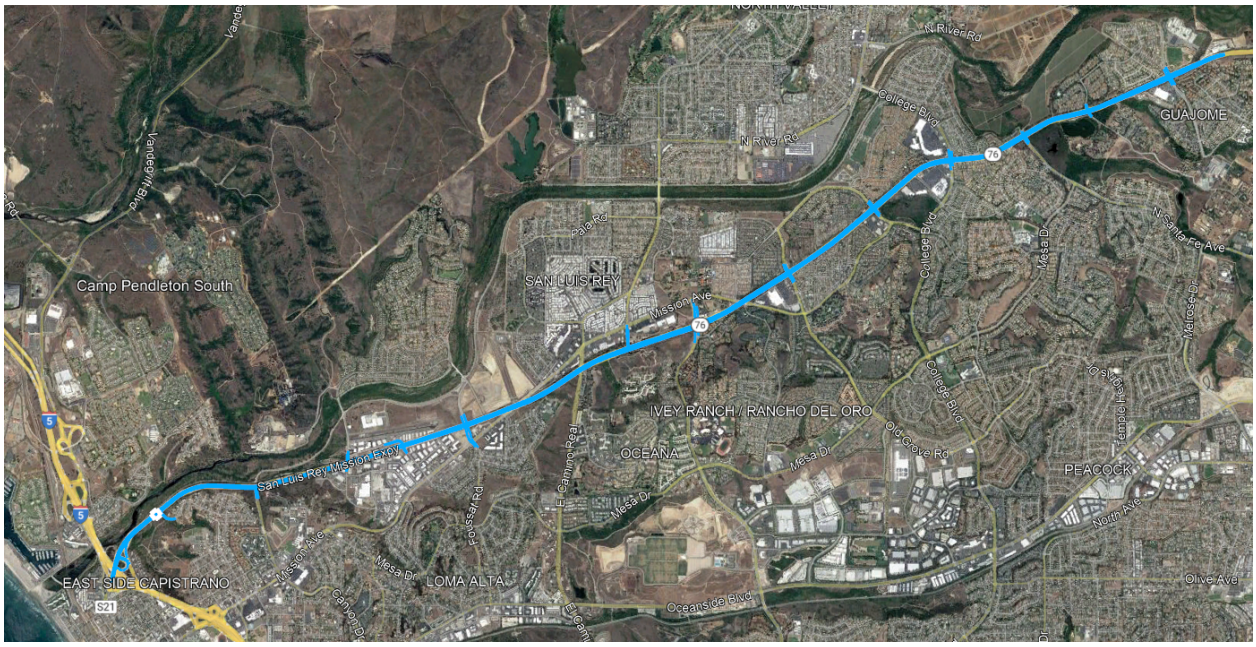

The total length is approximately 8.2 miles. The main roads were scanned four times and secondary roads were scanned twice.

2.2 Pre-Processing

Due to the large size and multiple overlapping scans in the original LAS dataset, preprocessing involves data partitioning and tiling to improve manageability and processing efficiency. This step ensures optimized storage, faster computation, and better handling in GIS and LiDAR processing software.

To facilitate processing, the dataset is divided into smaller tiles and each tile maintains a manageable size, allowing efficient processing without an expensive computational load.

Figure 2. Illustration of Subset Rectangle Boundaries of LAZ Files

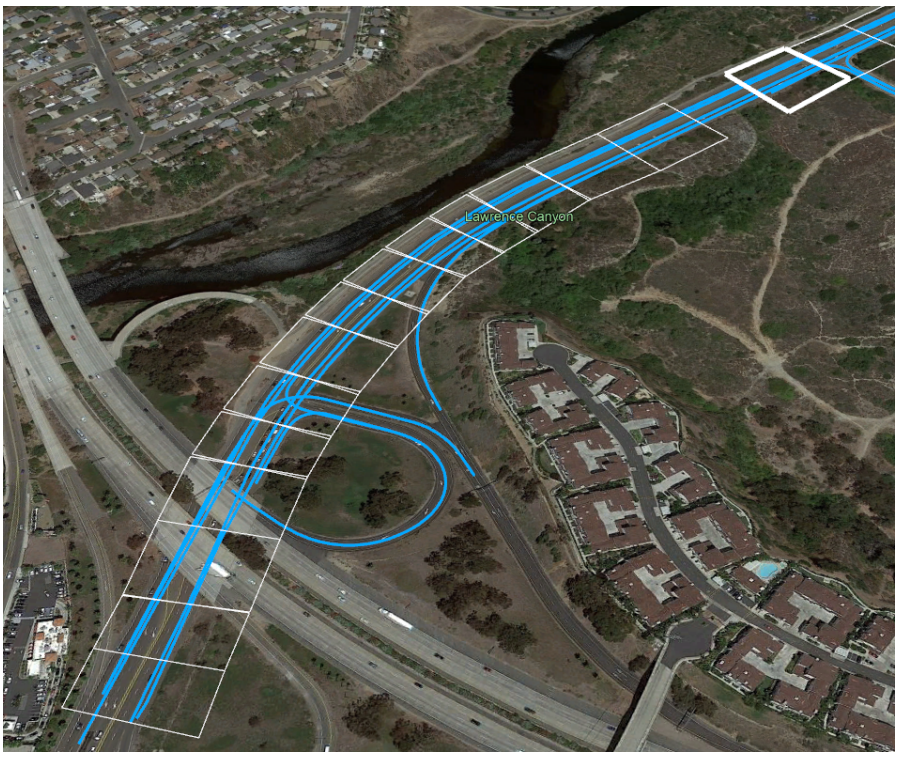

The width (distance across the road) is 250 ft to cover both lane and roadside features. Once points are extracted from the boundaries, multi-scans are merged to increase the point density and reduce the shadow effects where laser signals are blocked by features on roads such as road medians.

Figure 3. Example of Shadow Effect in Laser Scan

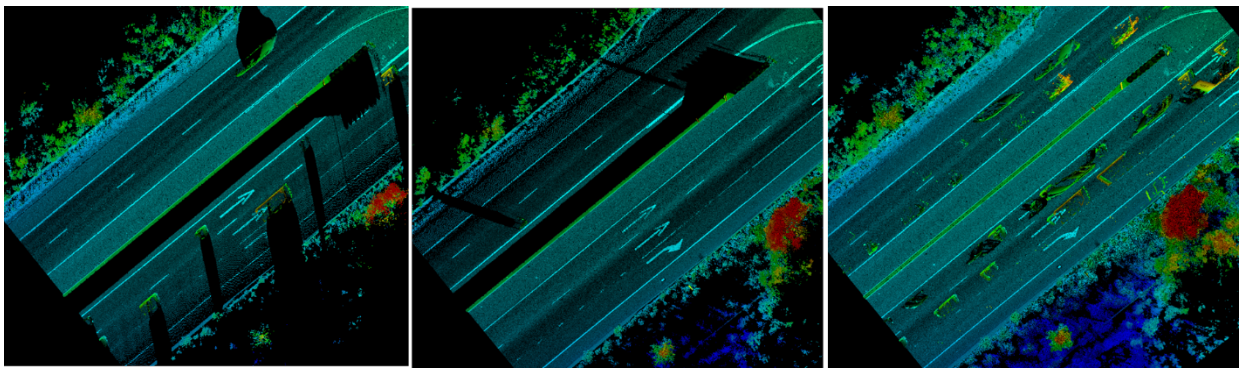

Left lane scan (left), right lane scan (middle), and combined point cloud (right).

Figure 3 illustrates the shadow effect where laser pulses are blocked by obstacles such as a median structure or other vehicles in the data acquisition stage. When merged with other scans, areas blocked by obstacles during one pass can often be filled in, as those obstacles may not be present in other passes. However, if the same obstacle is present in all scans, those areas may remain occluded and unobservable in the final dataset. Furthermore, merging increases the density of points which increases spatial resolution of point cloud data.

3. Roadside Assets

3.1 Road Lanes in MTLS Data

Road lane detection and extraction from Mobile Terrestrial Laser Scanning (MTLS) data play a crucial role in transportation management, autonomous navigation, and roadway maintenance (Williams et al., 2013). The extraction of road lane markings represents one of the most valuable applications of MTLS data processing.

MTLS provides high-density, georeferenced 3D point cloud data, enabling a detailed analysis of road markings, lane boundaries, and surface conditions. The ability to accurately identify road lanes from MTLS data enhances applications such as lane-level navigation, traffic monitoring, and intelligent transportation systems (ITS).

3.1.1 Characteristics of Road Lanes in MTLS Data

Road lanes in MTLS point clouds are typically identified using a combination of geometric, radiometric, and topological features. Based on Soilán et al. (2019), implementing a two-step process, road surface segmentation and intensity-based thresholding techniques were tested.

Key characteristics of road lane data include:

- Intensity Information – Lane markings, such as white and yellow stripes, exhibit distinct reflectance values in LiDAR intensity data, making them distinguishable from asphalt or concrete road surfaces.

- Elevation Consistency – Road lanes are generally located on a relatively uniform elevation, with minimal height variations compared to sidewalks or medians.

- Parallel Structures – Lanes usually follow parallel or structured paths, which can be detected using spatial clustering and feature extraction techniques.

- Curvature and Width – Road curvature and lane width measurements can be derived from point cloud analysis, supporting the identification of different road types (e.g., highways, local streets, intersections).

3.1.2 Segmenting road vs. non-road points

Separating bare-earth points from point cloud data is not new (Sithole and Vosselman, 2004; Pingel et al., 2013), and this concept has been extended to include the segmentation of road and non-road points. The accurate segmentation of road and non-road points represents a critical preprocessing step in mobile LiDAR data analysis for transportation applications. Among various

segmentation approaches, the “segmentGroundSMRF” function in MATLAB implements the Simple Morphological Filter (SMRF), which has proven particularly effective for processing mobile LiDAR and airborne LiDAR data to extract terrain surfaces.

SMRF applies mathematical morphology techniques to point clouds; specifically, the filtering operation it uses is conceptually equivalent to the “opening” operator in image processing. This approach first converts the irregular point cloud into a regular grid, then identifies ground points through a series of morphological operations and progressive thresholding. The algorithm's effectiveness stems from its ability to adapt to local terrain variations while maintaining computational efficiency.

The process involves several key steps:

- Conversion of the 3D point cloud to a 2.5D height raster
- Application of an opening operation with a progressively larger structural element
- Identification of ground points based on elevation thresholds relative to the morphologically processed surface
- Classification of remaining points as non-ground features

Figure 4. Ground Points, Non-Ground Points, and Original Point

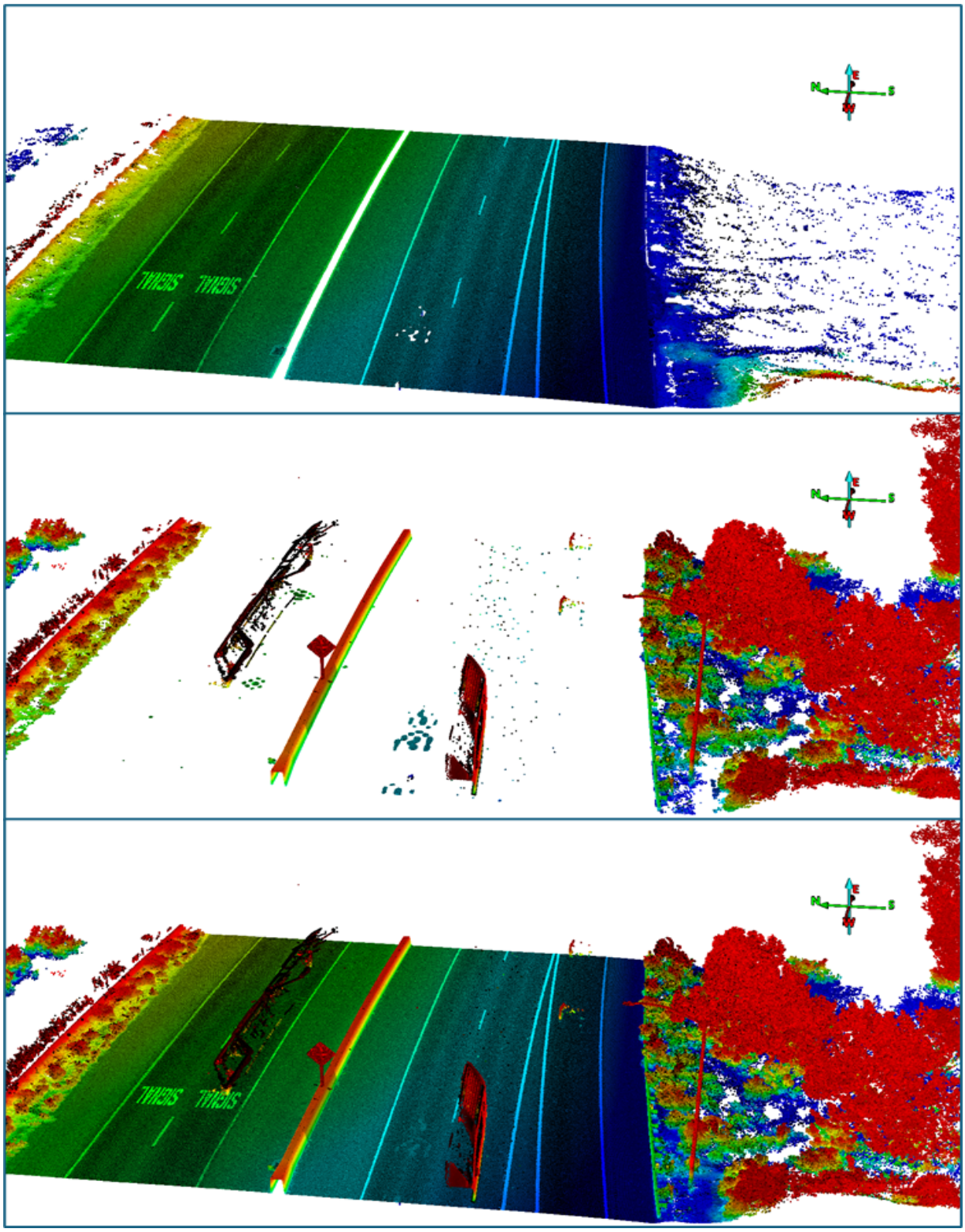

Ground points (upper), non-ground points (middle), and original point (lower).

Figure 4 illustrates the segmentation of ground and non-ground points. The segmentation clearly distinguishes ground points (predominantly road surface) from non-ground elements. The ground points comprise the road surface, shoulders, and adjacent terrain with consistent elevation changes. Non-ground points encompass vegetation, road median structures, traffic signs, utility poles, and what are commonly referred to as "ghost points"—false data points typically generated by moving vehicles near the LiDAR scanner during data acquisition.

3.1.3 Raster Data from Point Cloud

In the processing workflow of mobile LiDAR point clouds, generating a Digital Elevation Model (DEM) and intensity raster map is crucial step for terrain analysis and feature extraction. This step transforms the raw 3D point cloud data into structured 2D raster representations, enhancing interpretability and usability for various applications. In this report, two types of raster data are generated: (1) Digital Elevation Model (DEM) and (2) Intensity Map. Once raster data is generated, 2D image processing tools can be applied to extract features such as lanes.

Digital Elevation Models from Point Clouds

Digital Elevation Models (DEMs) derived from mobile LiDAR data provide highly accurate representations of the bare-earth surface, making them indispensable for applications such as transportation planning, flood modeling, and infrastructure design. Mobile LiDAR systems capture dense point clouds with centimeter-level precision, enabling detailed elevation mapping even in complex urban environments. The conversion of irregular point clouds into DEMs involves interpolation techniques, such as Natural Neighbor or Triangulated Irregular Network (TIN), to ensure smooth and accurate terrain representation. These methods are particularly effective in areas with varying point densities and terrain complexity, allowing for the extraction of features such as road surfaces and drainage patterns.

The mobile LiDAR has 400–500 points per square feet, which translates to 4300–5400 points per square meters. Assuming uniform distribution, one can use an equation (Hu, 2023) that defines the grid resolution, given the point density, for the DEM,

$$DEM\ resolution = \sqrt{\frac{1}{N}} \text{ ---- (1)}$$

where N is the point density, i.e., the number of points per unit area. For example, when there is 1 point per square meter, the optimal DEM resolution will be 1 meter (Garzon et al., 2021).

With a point density of 400–500 points per square foot (~4300–5400 pts/m^2), one can theoretically generate a DEM with a resolution of 1.3–1.5 cm. However, to balance detail and surface smoothness, DEMs with a resolution of 2–5 cm are typically used for roadside asset mapping and

surface modeling. In this research, 0.1 feet (or 3.038 cm) was generated; a 3 cm spatial resolution can effectively detect road features such as slopes, lanes, median structures, and more.

Intensity Raster Generation

Unlike elevation data, intensity values in LiDAR returns represent the reflectivity of surfaces to the emitted laser pulse. As noted by Vosselman (2002), these values are influenced by multiple factors including:

- Surface material properties
- Incidence angle
- Range to target
- Environmental conditions
- Sensor-specific calibration

Pfeifer et al. (2007) demonstrated that intensity values require normalization to account for the range dependency before generating comparable intensity rasters. Their proposed correction model adjusts raw intensity values based on the inverse square distance relationship, significantly improving the consistency of intensity representation across the scan.

For road marking detection, Yang et al. (2020) developed a dual-threshold intensity rasterization technique that enhances the contrast between road surfaces and highly reflective markings. Their approach dynamically adjusts cell values based on local intensity statistics, achieving 92% detection accuracy for lane markings in varying illumination conditions.

Figure 5. Digital Elevation Model and Intensity Map

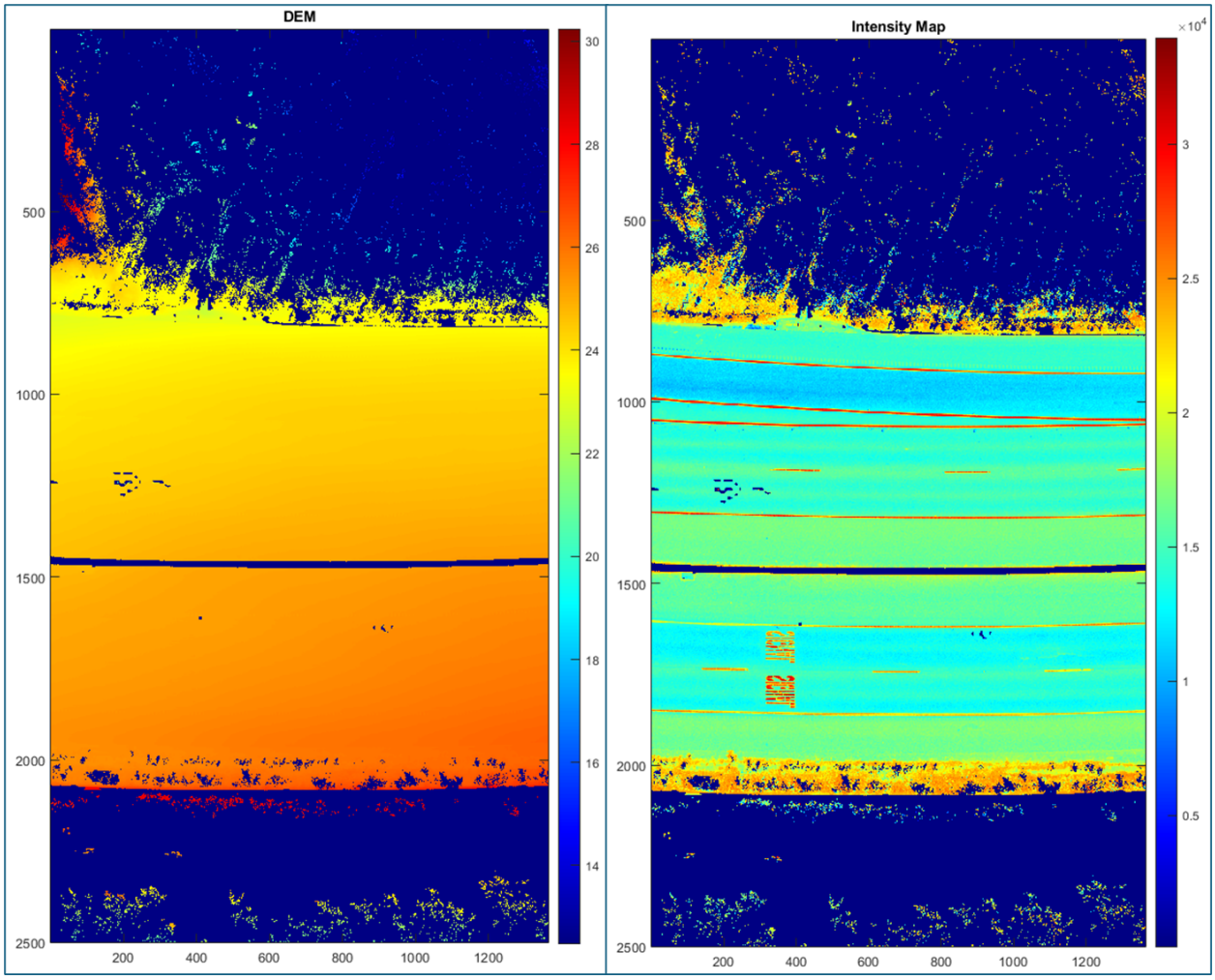

Digital Elevation Model (left) and Intensity Map (right) from rasterization of point clouds.

As illustrated in Figure 5, while the DEM clearly represents the flat and smooth topography of the road surface with elevation changes at curbs and medians, the intensity map reveals detailed information about surface materials and markings not apparent in the elevation data. The high reflectivity of thermoplastic or paint-based road markings creates a stark contrast against the asphalt background, facilitating automated feature extraction.

Importantly, the resolution adequacy differs between these two raster types. Road geometry analysis typically requires DEM resolutions of 10–15 cm, while intensity-based feature extraction benefits from higher resolutions of 2–5 cm to capture fine details such as dashed lane markings and symbols. In this study, Intensity maps have the same resolution of 3 cm as in the DEM.

3.1.4 Road Lane Extraction

The extraction of road lane markings from mobile LiDAR data represents a critical component in roadway analysis, autonomous navigation, and infrastructure management. This section details the methodological approach employed to identify and delineate lane markings using intensity information derived from point cloud data.

Intensity-Based Thresholding

The initial phase of lane marking extraction utilizes the distinct reflective properties of road markings compared to the surrounding pavement. As noted by Guan et al. (2014), pavement markings typically exhibit significantly higher retro reflectivity than asphalt or concrete surfaces, creating a distinctive intensity signature in LiDAR returns.

In our processing workflow, an intensity threshold of 18000 was empirically determined to effectively isolate potential lane marking pixels. This approach aligns with research by Kumar et al. (2013), who demonstrated that adaptive thresholding based on intensity histograms can achieve marking detection rates exceeding 90% in various lighting and weather conditions. Their work established that while absolute intensity values vary between different LiDAR systems, the relative contrast between markings and road surfaces remains consistent enough for threshold-based separation.

Yu et al. (2015) further validated this approach, showing that, for typical thermoplastic road markings, intensity returns are approximately 2.5–3.5 times higher than surrounding asphalt, creating a bimodal distribution in intensity histograms that facilitates separation. However, as cautioned by Soilán et al. (2017), worn markings or wet surface conditions can reduce this contrast, potentially requiring locally adaptive thresholds rather than global values.

Binarization and Edge Detection

Following intensity thresholding, the resulting raster undergoes binarization to create a black and white image suitable for edge detection algorithms. This transformation simplifies the continuous intensity values into a binary representation where road markings are isolated from the background.

For edge detection, the Sobel operator was selected due to its computational efficiency and effectiveness in detecting strong gradients characteristic of lane marking boundaries. Sobel edge detection performs particularly well for linear features in rasterized LiDAR data, offering superior noise rejection compared to simpler gradient operators.

The Sobel operator computes the approximate gradient of image intensity at each pixel by convolving the image with two 3×3 kernels that estimate derivatives in the horizontal and vertical

directions. With robustness and simplicity, the Sobel operator (Cao et al., 2019; Javeed et al., 2024) is used as pre-processing for detecting linear features.

Figure 6. Black and White Image (upper left), Sobel Edge Image (lower left), and Road Lane Detected (right)

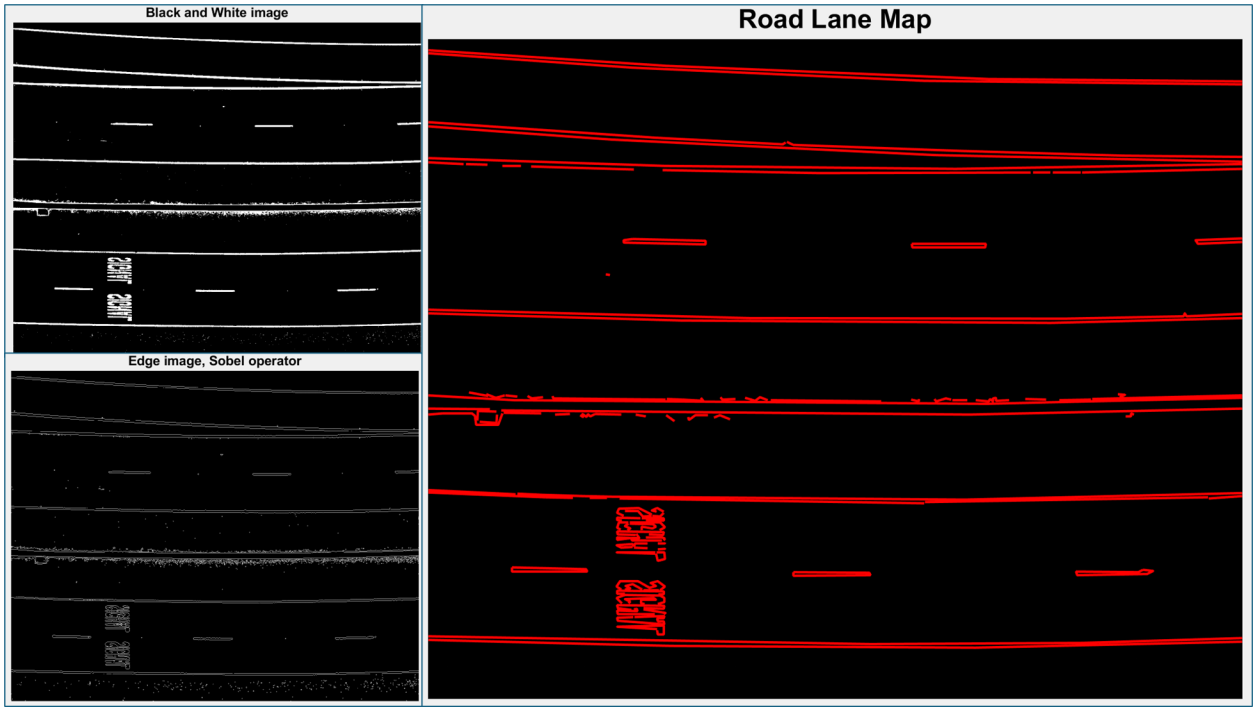

Line Fitting and Segment Connection

To refine the edge detection results and eliminate noise, a length-based filtering approach was implemented. Specifically, edge segments shorter than 20 pixels were removed, preserving only substantial linear features that potentially represent lane markings. Following length filtering, the Hough transform technique was applied to fit straight lines to the remaining edge segments. The Hough transform is particularly well-suited for identifying linear patterns in noisy binary images by converting the image space into a parameter space where lines are represented as points.

For connecting discontinuous segments belonging to the same lane marking, a proximity and orientation-based clustering algorithm was implemented. Segments with similar orientation (within ±5°) and proximity (gap < 2 meters) were grouped and connected to form continuous lane representations. This process is particularly important for dashed lane markings, where gaps between paint segments must be bridged to create a complete lane model.

Figure 7. Road Lanes Extracted from 3 Tiles of Data (upper) and
Google Earth Pro Image of Said Road

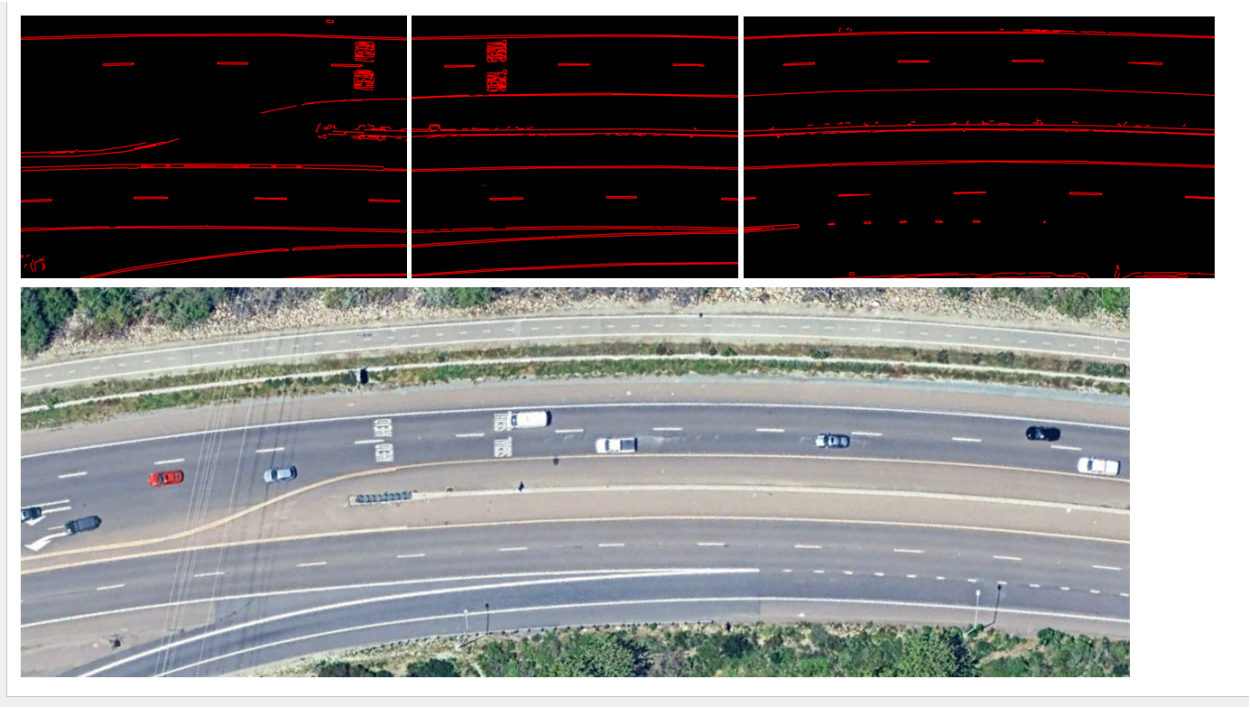

As illustrated in Figure 7, the extracted lane markings closely correspond to the actual road configuration visible in the Google Earth imagery. The algorithm successfully identified both solid and dashed lane markings, as well as edge lines delineating the road boundaries.

3.2 Cross Section Slope Analysis on the Road

Slope analysis is a critical component in road infrastructure assessment, ensuring proper drainage, vehicle stability, and pavement longevity. Mobile LiDAR (Light Detection and Ranging) provides high-density 3D point cloud data, enabling precise measurement of road cross-sections and slopes.

Traditional survey methods for measuring cross slopes are time-consuming and limited in accuracy. Mobile LiDAR technology provides high-resolution 3D point cloud data, enabling precise and efficient extraction of road cross-sections and slope measurements. By analyzing road slope variations, engineers can assess compliance with design standards, detect potential drainage issues, and identify areas susceptible to erosion or structural failure.

According to California Department of Transportation Highway Design Manuals and Federal Highway Administration Guidelines, road cross-slope values typically range from 1.5% to 2.5% for standard highways, with these values carefully specified in design guidelines to balance water drainage against vehicle stability. Deviations from these standards can lead to hydroplaning risks,

increased accident rates, and accelerated pavement deterioration. The high precision of mobile LiDAR data.

3.2.1 Methodology for Cross-Section Slope Analysis

The process of cross-section slope analysis from mobile LiDAR data involves several key steps, each critical to ensuring accurate results. According to Gargoum and El-Basyouny (2019), a systematic workflow is essential to minimize errors and ensure consistency across the analyzed road segments.

Noise Removal and Data Preparation

The initial phase involves eliminating irrelevant or erroneous data points to enhance accuracy. Noise in mobile LiDAR data typically arises from multiple sources, including:

- Moving objects captured during scanning (vehicles, pedestrians)
- Multi-path reflections from highly reflective surfaces
- Atmospheric interference
- Scanner measurement errors

Effective noise removal requires a combination of statistical outlier detection and contextual filtering. To enhance LiDAR point cloud denoising in MATLAB, the integration of "pcmedian" and "pcdenoise" provides a robust approach to filtering noise while preserving structural details. "pcmedian" applies a median filter to smooth intensity or depth variations, making it particularly useful for reducing speckle noise in airborne or terrestrial LiDAR scans. "pcdenoise," on the other hand, leverages statistical outlier removal and radius-based filtering to eliminate sparse noise and improve classification accuracy.

By combining these methods, "pcmedian" can refine point attributes before applying "pcdenoise" to remove outliers, ensuring a cleaner dataset for segmentation and feature extraction. This multi-step denoising process enhances LiDAR-based terrain modeling, urban mapping, and object recognition by reducing false classifications caused by noise artifacts.

Ground Point Extraction

Ground points were separated from non-ground points using the Simple Morphological Filter (SMRF) method. This step was crucial for isolating the road surface, enabling the accurate measurement of slopes and elevation profiles. Key parameters such as window radius, slope threshold, and elevation threshold were adjusted to enhance the accuracy of ground classification. The SMRF approach applies progressive morphological operations to identify ground points based

on local elevation variations. MATLAB provides the built-in function "segmentGroundSMRF" for segmenting ground points from LiDAR point cloud.

Digital Elevation Model (DEM) Creation

A DEM was generated at a fine grid resolution to represent the terrain accurately. The DEM served as a reference for extracting elevation values along the road cross-sections and assessing slope variations. The simple bin algorithm (Kim et al., 2006) was implemented in MATLAB.

Road Centerline Definition

The road centerline was defined interactively to serve as the baseline for extracting cross-sections. This approach allowed for accurate alignment of cross-section profiles perpendicular to the direction of the road, ensuring consistent slope measurements. While manual centerline definition provides high accuracy, automated approaches have been developed to increase efficiency.

Cross-Section Extraction and Analysis

Cross-sections were extracted at regular intervals along the road centerline. Each cross-section spanned the full width of the road and consisted of multiple sample points to capture detailed elevation profiles. The analysis involved computing slope values for both left and right sides of the road at each cross-section. The extraction process involves defining profile lines perpendicular to the road centerline and sampling elevation values along these profiles.

Elevation Profiling and Slope Analysis

Elevation profiles were generated for the left and right sides of each cross-section. Mean elevation differences between the two sides were calculated to identify potential drainage issues or uneven pavement conditions. Slope values were analyzed to assess compliance with design standards and to detect areas susceptible to erosion or water accumulation.

According to the American Association of State Highway and Transportation Officials (AASHTO), typical values for cross-section slope fall within the following ranges:

- Asphalt/concrete pavements: 1.5%–2%
- High-speed highways: 1.5%–2.5%
- Urban roads: 2%–3%

Figure 8. Illustration of Cross-Section Extraction Scheme

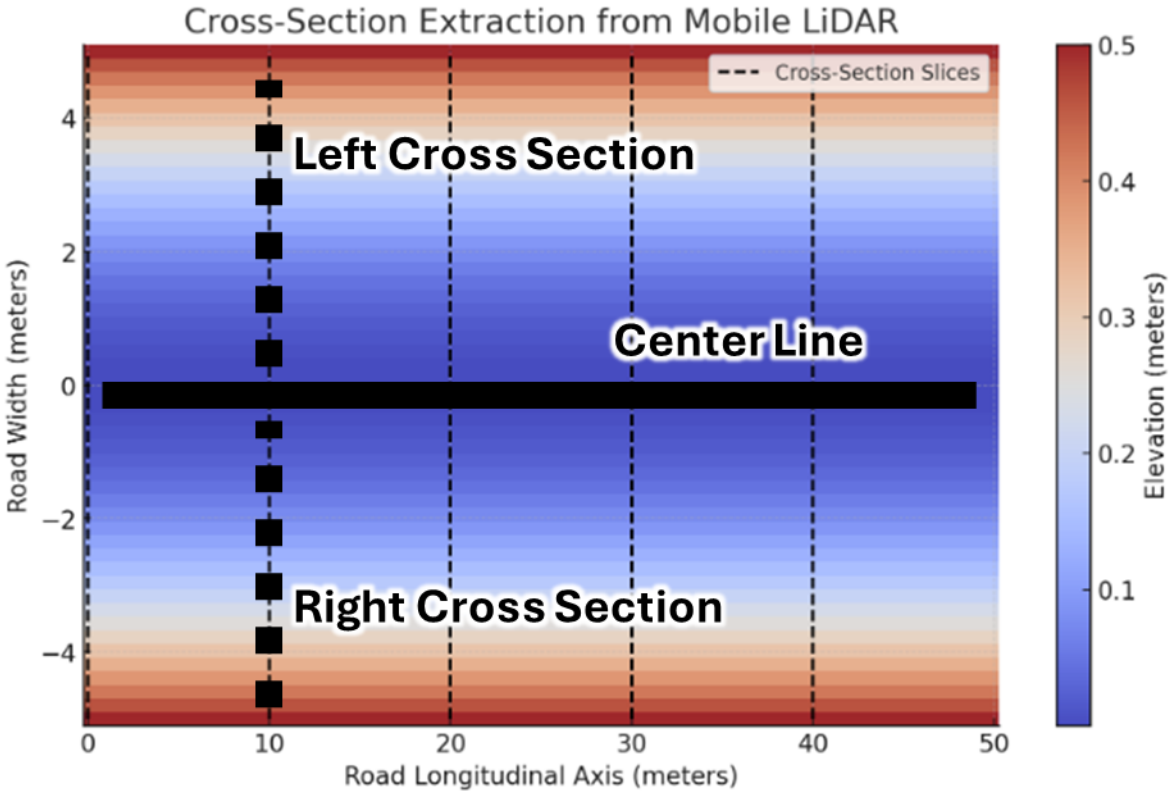

Figure 8 illustrates the scheme of center line and left/right cross-section extraction. The road is divided into equal intervals (e.g., every 5–10 meters) along its longitudinal axis. At each interval, a perpendicular cross-section slice of LiDAR points is extracted. Each slice consists of elevation (Z) values corresponding to different lateral positions across the road width.

3.2.2 Testing 3 tiles for Cross-Section Profile Analysis

Three tiles with different curvatures—one straight line and two curved lines—were proceeded, and their cross-section profiles were analyzed. The road center was manually digitized. Cross-section spacing is 20 ft; 50 ft left and right profiles were created and the sampled 1 ft.

Test 1: Straight Road, 12 Profiles

Figure 9. Cross-Section Profile Test 1

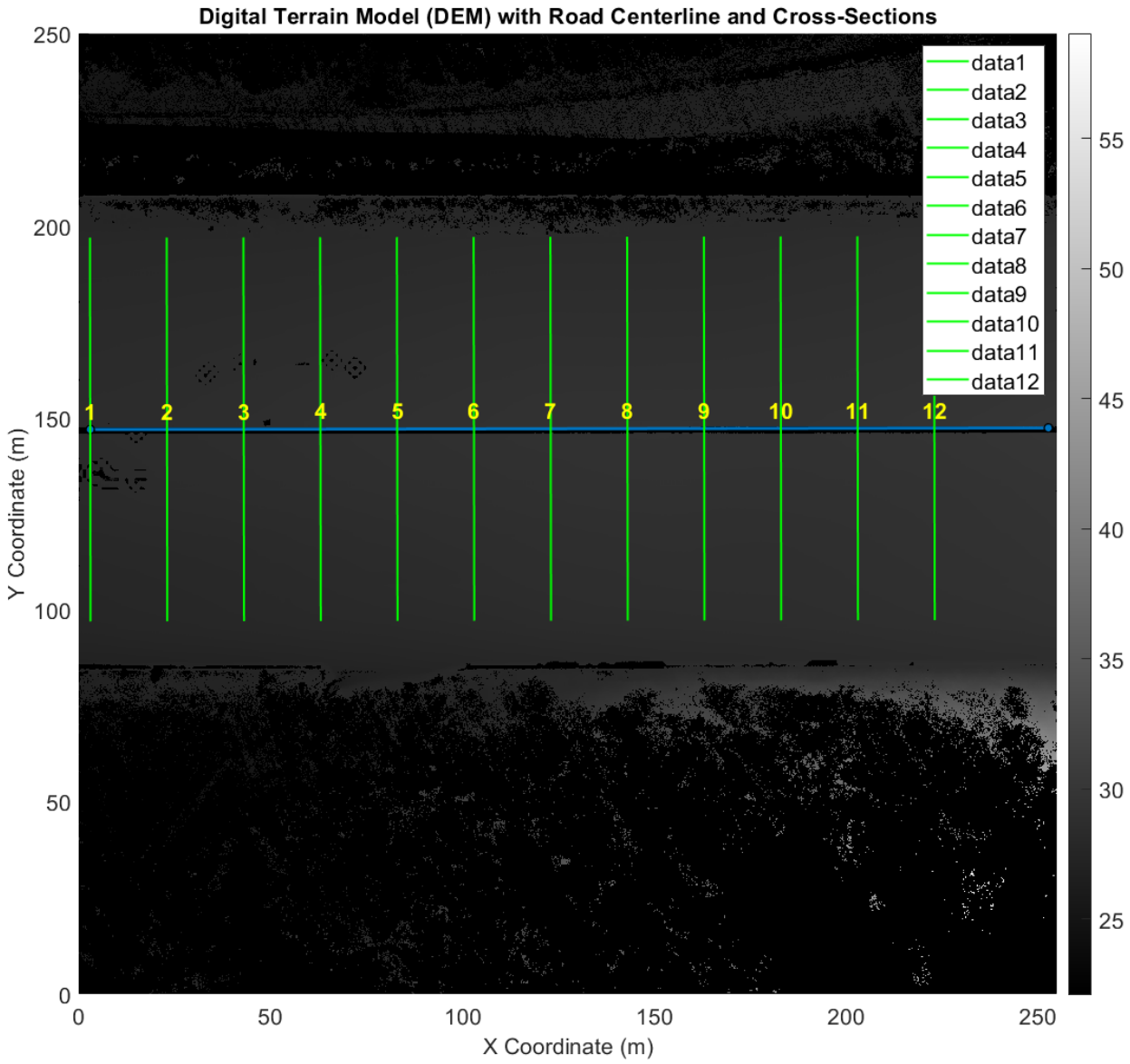

Figure 10. Cross-Section Profile Test 1, 3D View

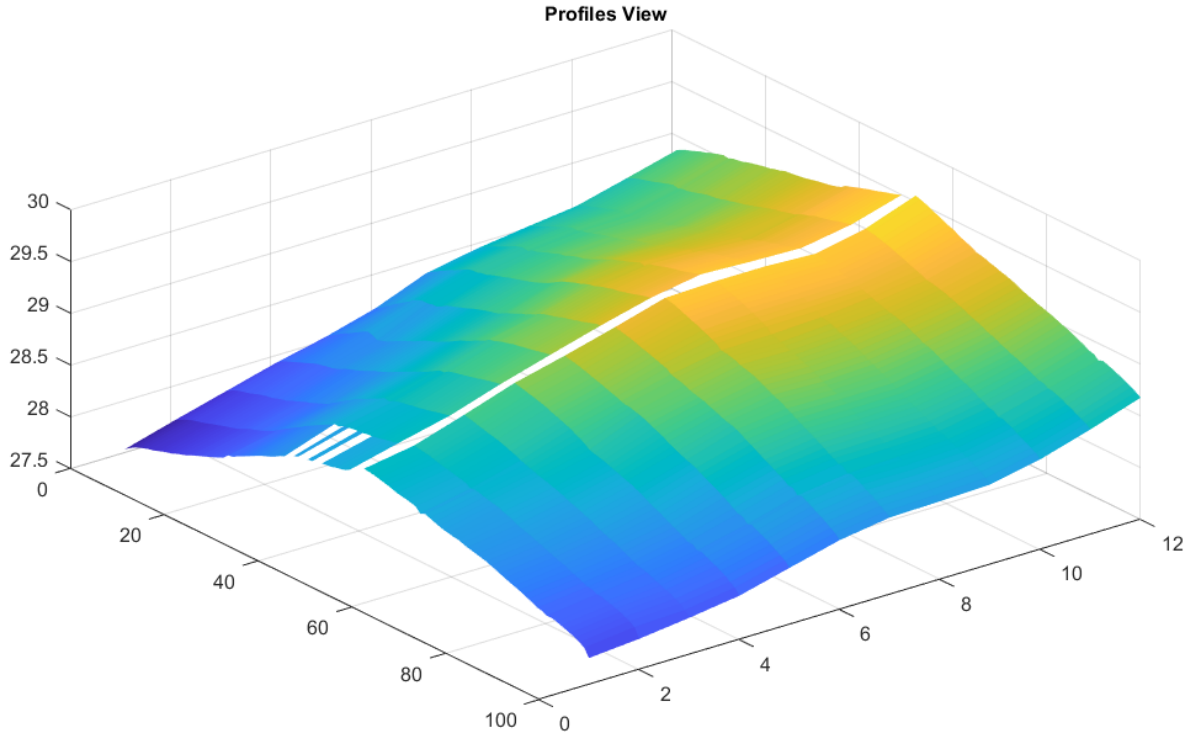

Table 1. Cross-section Profile Test 1 Result

Cross-Section Index	Left Slope (%)	Right Slope (%)
Cross-Section 1	1.435	-1.869
Cross-Section 2	1.522	-1.920
Cross-Section 3	1.764	-1.869
Cross-Section 4	1.980	-1.861
Cross-Section 5	2.015	-1.909
Cross-Section 6	2.010	-1.783
Cross-Section 7	2.153	-1.679
Cross-Section 8	2.175	-1.645
Cross-Section 9	2.144	-1.469
Cross-Section 10	1.940	-1.333
Cross-Section 11	1.801	-1.258
Cross-Section 12	1.760	-1.215

Test 2: Curved Road, 9 Profiles

Figure 11. Cross-Section Profile Test 2

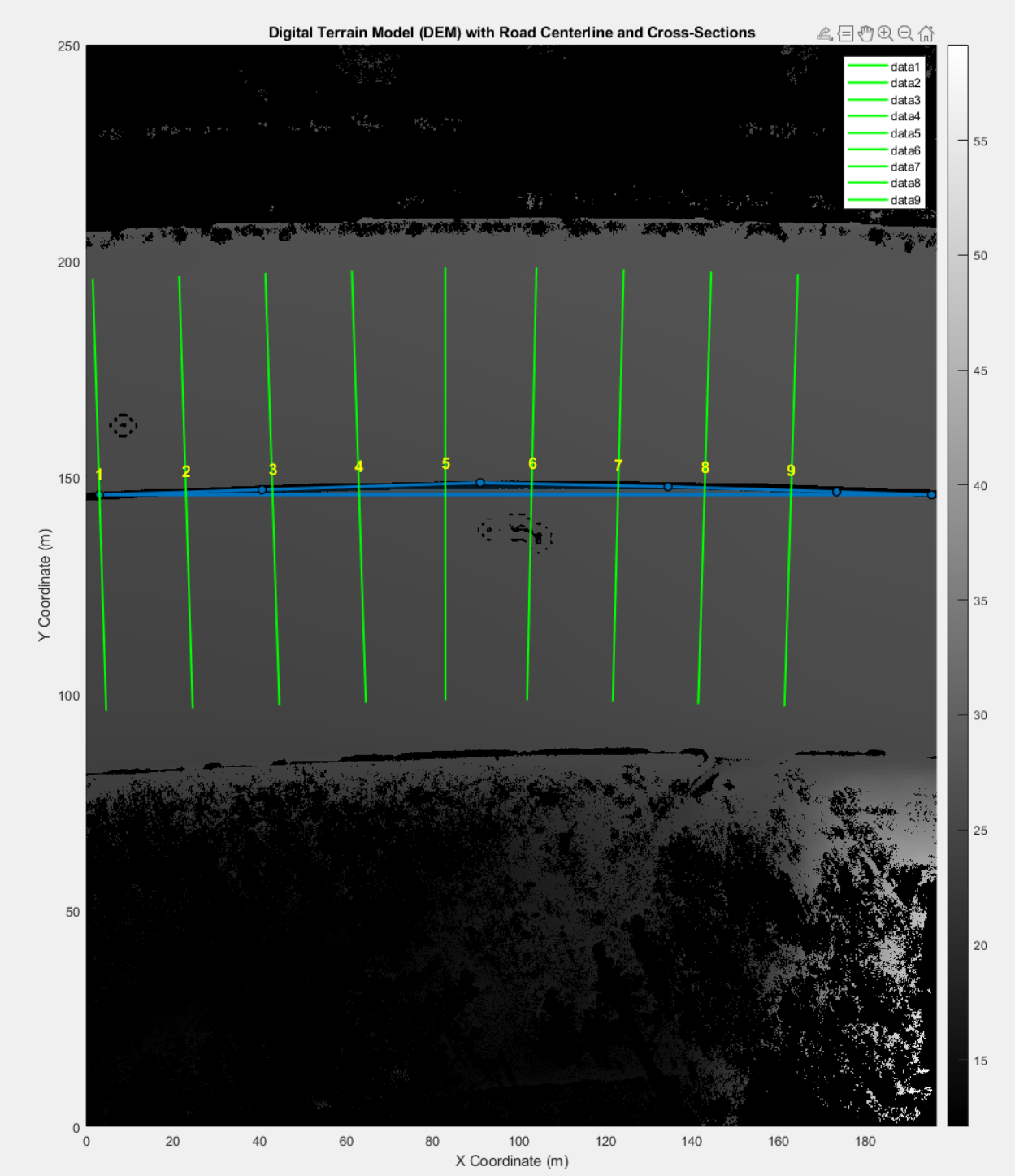

Table 2. Cross-section Profile Test 2 Result

Cross-Section Index	Left Slope (%)	Right Slope (%)
Cross-Section 1	-1.958	-2.080
Cross-Section 2	-2.195	-1.994
Cross-Section 3	-2.326	-1.959
Cross-Section 4	-2.315	-2.039
Cross-Section 5	-2.315	-2.000
Cross-Section 6	-2.356	-1.918
Cross-Section 7	-2.169	-1.827
Cross-Section 8	-1.877	-1.750
Cross-Section 9	-1.590	-1.830

Test 3: Slight Curved Road, 12 Profiles

Figure 12. Cross-Section Profile Test 3

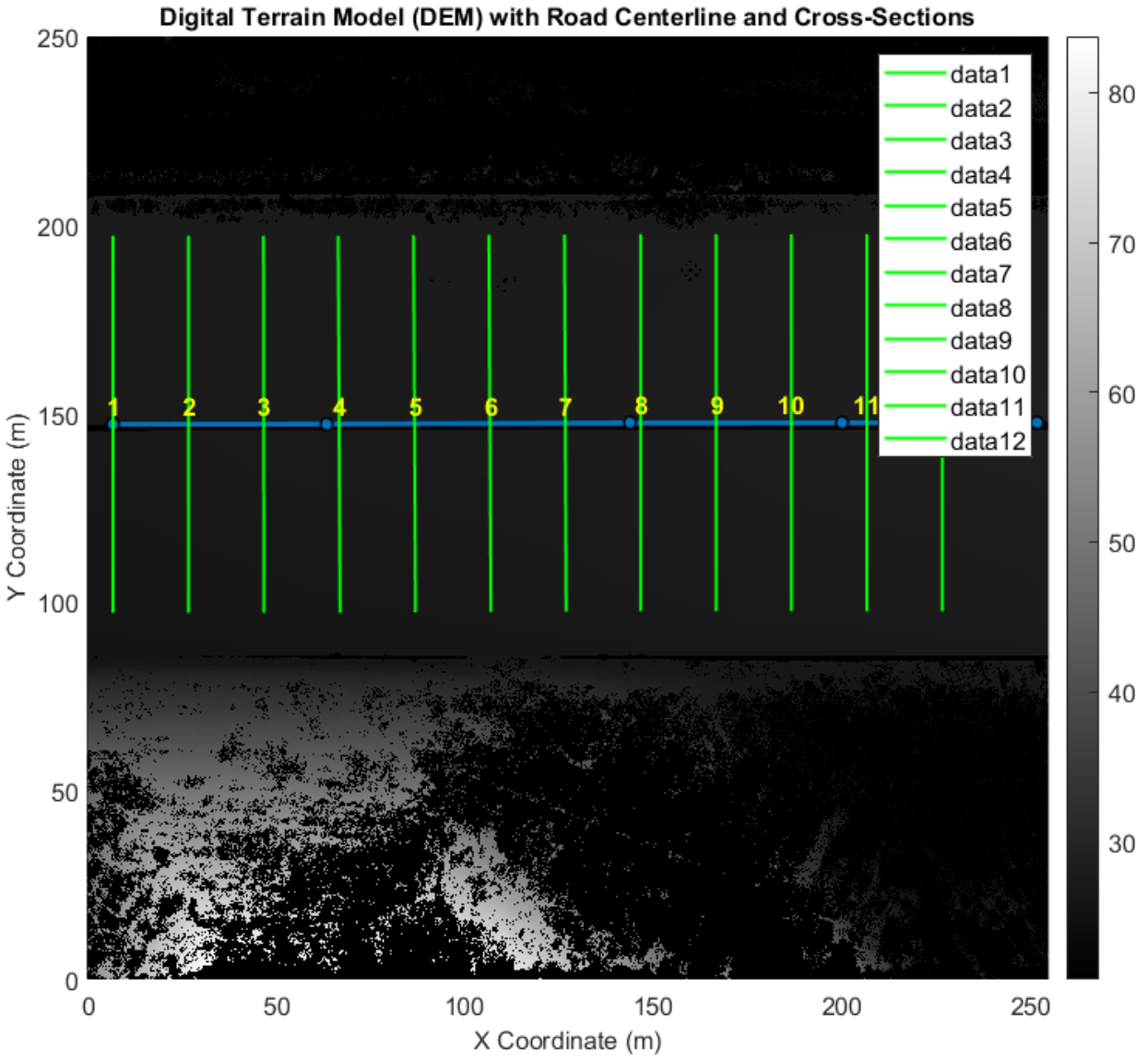

Table 3. Cross-section Profile Test 3 Result

Cross-Section Index	Left Slope (%)	Right Slope (%)
Cross-Section 1	-1.307	-1.798
Cross-Section 2	-1.163	-1.844
Cross-Section 3	-0.927	-1.874
Cross-Section 4	-0.802	-1.782
Cross-Section 5	-0.690	-1.720
Cross-Section 6	-0.462	-1.633
Cross-Section 7	-0.218	-1.599
Cross-Section 8	0.027	-1.622
Cross-Section 9	0.329	-1.731
Cross-Section 10	0.545	-1.846
Cross-Section 11	0.837	-1.910
Cross-Section 12	1.128	-1.976

Figure 13. Results of Three Cross-Sections

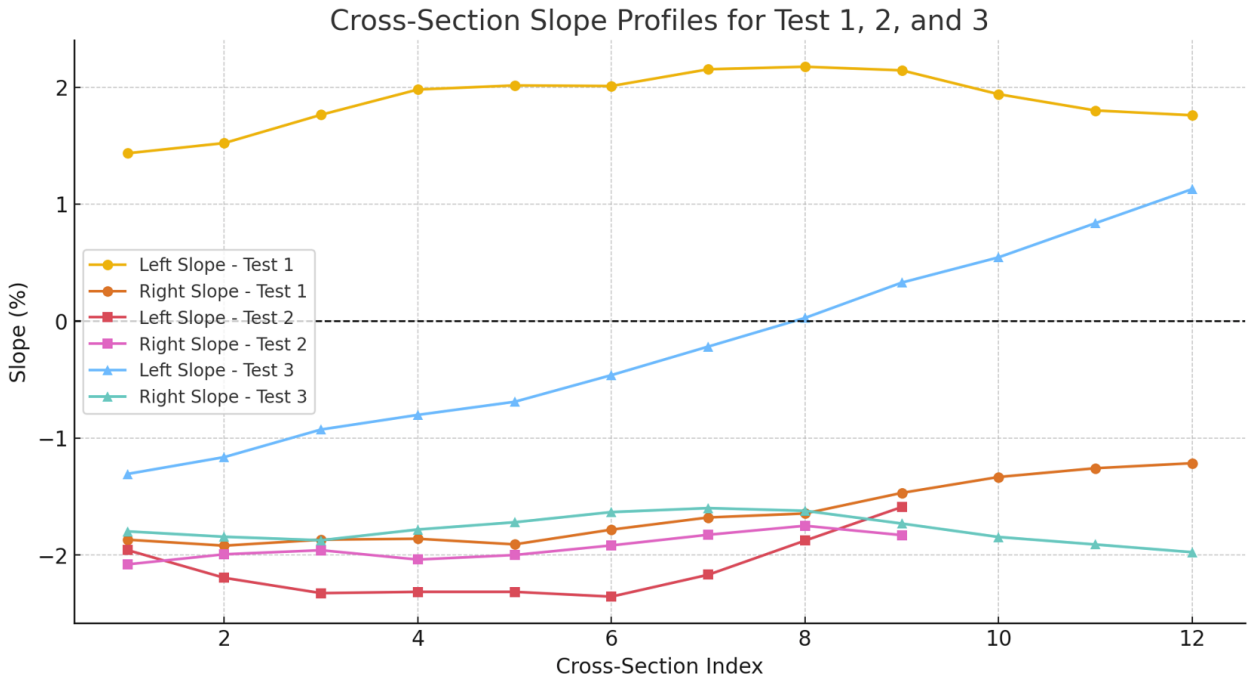

In Test 1 (straight road), the left slope (1.89% mean) and right slope (-1.65% mean) indicate a typical crowned road profile, where the pavement is higher in the center and slopes downward toward both edges to facilitate proper drainage. This is a common design feature for straight roads, preventing water accumulation and minimizing hydroplaning risks.

The relatively low standard deviation (~0.24% left, ~0.27% right) suggests that the cross slopes are consistent across all sections, meaning the road maintains a uniform transverse slope without significant deformations.

Test 2 (curved road) shows a superelevated slope, which is expected in curved roadway designs to ensure vehicle stability and drainage efficiency. The negative left slope (-2.12%) and slightly less steep right slope (-1.93%) indicate a properly implemented superelevation, where the entire road surface is banked towards the curve's center to counteract centrifugal forces.

Test 3 (slightly curved road) being in the transition phase of superelevation. In the early stages of superelevation, the left slope starts off relatively flat (-0.22% mean), gradually increasing towards positive values (1.13% at cross-section 12). This gradual shift indicates the beginning of roadway banking, where the left side is slowly being raised to match the designed superelevation profile.

3.3 Assessment of Existing LiDAR Point Cloud Processing Programs

This section evaluates existing LiDAR point cloud processing programs, focusing on Trimble Business Center (TBC) (Trimble Inc.), Global Mapper Pro (GMP) (Blue Marble Geographics), and Cyclone 3DR (Leica Geosystems). The assessment examines their strengths, limitations, and overall effectiveness in point cloud classification, feature extraction, and user experience to determine the most suitable tool for processing mobile LiDAR data for road infrastructure analysis. While ArcGIS Pro also offers point cloud processing capabilities, its functionality remains limited, particularly in detailed classification tasks such as segmenting ground, buildings, and vegetation.

Trimble Business Center (TBC)

The Trimble Business Center (TBC) serves as a comprehensive software solution for point cloud processing, accommodating various data acquisition methods including mobile, aerial, and terrestrial LiDAR systems, as well as tunnel survey data (Trimble Inc.). The platform leverages machine learning techniques to facilitate accurate point cloud classification while maintaining computational efficiency.

The software's classification system employs artificial intelligence algorithms that effectively extract relevant features from heterogeneous point cloud datasets, enhancing the analysis capabilities across both terrestrial and aerial LiDAR. TBC offers refined filtering mechanisms and expanded classification parameters that enable users to perform detailed segmentation of point clouds with increased automation and customization options. In alignment with advancements in the reality capture sector, TBC continues to evolve its machine learning classification algorithms to improve accuracy and processing efficiency for LiDAR-based mapping and surveying applications.

Figure 14. Trimble Business Center Point Cloud Processing Menu

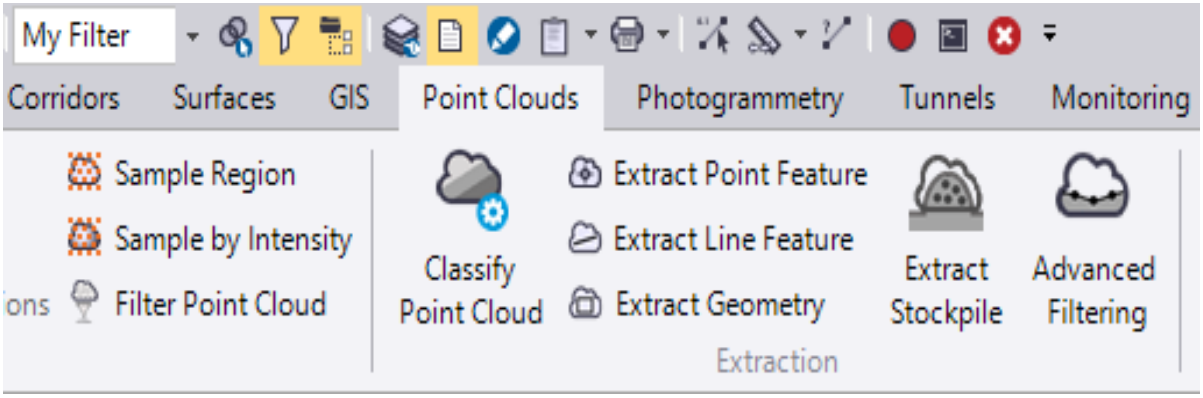

Figure 15. Result of Trimble Business Center (TBC) Deep Learning Point Cloud Classification

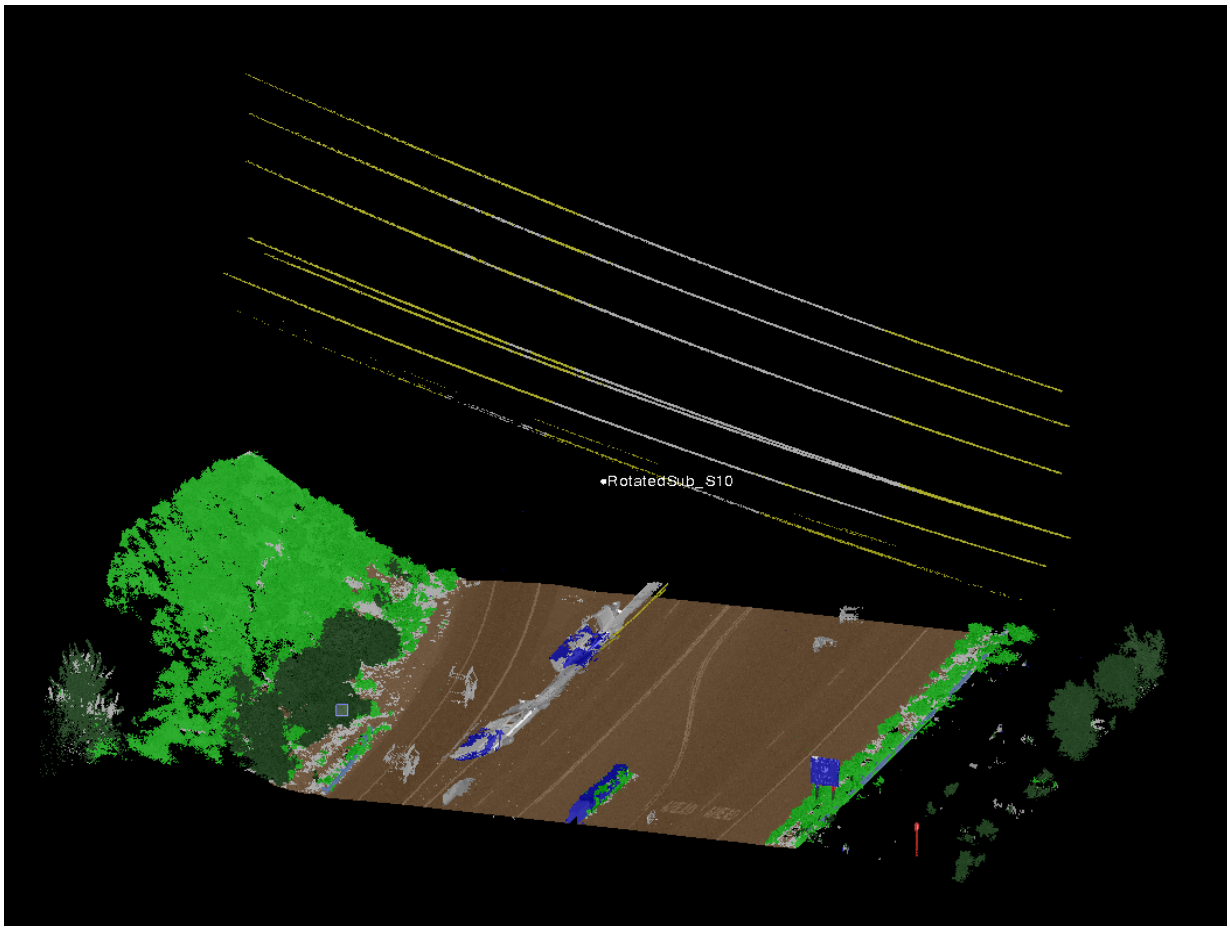

TBC exhibits notable accuracy in the classification of ground surfaces and structural elements, including buildings and median dividers. The software demonstrates particular effectiveness in semi-automatic road marking detection.

However, TBC shows limitations in overhead power line detection, with lower classification accuracy compared to Global Mapper Pro (GMP) when processing conductor points. Users frequently need to implement manual corrections through the Add to Region functionality to address misclassified point clusters. The software's performance remains unevaluated in scenarios with moderate to dense vegetation cover. Additionally, TBC encounters challenges when processing abbreviated lane markings and navigating the complexity of road intersections.

In summary, TBC proves most valuable for urban infrastructure classification applications, with particular strength in road feature extraction workflows, while demonstrating comparative weakness in power line segmentation tasks. The system does not provide complete automation, as manual refinement during post-processing is typically necessary to optimize classification results.

Global Mapper Pro (GMP)

Global Mapper Pro (GMP) employs a methodical, automated workflow architecture designed to optimize the point cloud classification process (Blue Marble Geographics). The software places particular emphasis on efficient detection and classification of power infrastructure, including transmission lines and supporting poles. In contrast to TBC, GMP provides users with a more streamlined interface that reduces complexity while maintaining essential functionality.

The platform's automated classification system follows a sequential approach that guides users through standardized processing steps, facilitating consistent results across different operators and projects. GMP's specialization in power corridor analysis is evident in its dedicated algorithms for overhead conductor detection and pole classification. This specialized focus complements its accessible user interface, which prioritizes operational simplicity without sacrificing processing capabilities relevant to utility corridor mapping and analysis.

Figure 16. Global Mapper LiDAR Processing Menu

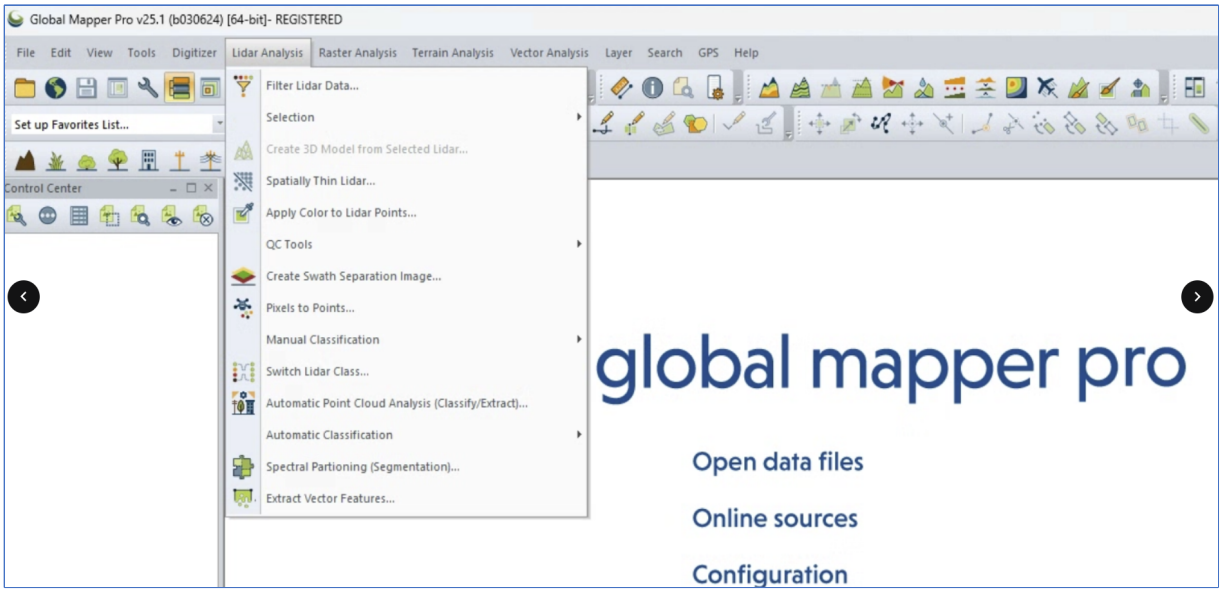

The classification tools in GMP follow a recommended sequential order, beginning with noise removal, followed by ground classification, building and vegetation detection, power line segmentation, and, finally, power pole identification (Blue Marble Geographics). This sequence is automatically applied when multiple classifications are selected simultaneously. The order is crucial because certain classifications rely on pre-processed data—for instance, the building and vegetation classifiers depend on accurately classified ground points to determine elevation differences.

GMP excels in power line detection, accurately identifying wires and conductors, making it particularly useful for analyzing utility infrastructure. It also demonstrates high accuracy in classifying ground points, ensuring reliable terrain modeling. Additionally, GMP offers an automated classification workflow, which minimizes manual corrections and enhances usability.

Despite its strengths, GMP performs exceptionally well in power line and ground classification but struggles with distinguishing poles from transmission towers, occasionally leading to errors in complex infrastructure mapping. The software requires careful parameter adjustments—particularly for Mobile Terrestrial Laser Scanning (MTLS) datasets—to maintain classification accuracy. Additionally, although GMP's efficient automated workflow simplifies processing, it offers less customization compared to TBC.

Cyclone 3DR

Cyclone 3DR, developed by Leica Geosystems, is a point cloud processing software designed for automatic classification and feature extraction (Leica Geosystems). It integrates AI-based object recognition and supports structured and unstructured LiDAR datasets. The software combines

advanced segmentation algorithms with machine learning techniques to facilitate efficient point cloud analysis across various application domains.

Cyclone 3DR's object recognition capabilities leverage convolutional neural networks trained on extensive point cloud datasets, enabling accurate identification of common infrastructure elements and natural features. This approach allows the software to process both organized point clouds from static terrestrial scanners and the more complex unstructured data typically generated by mobile LiDAR systems. The platform's integrated workflow supports a comprehensive range of processing tasks from initial registration to final feature extraction and modeling.

The software's classification system employs contextual analysis that considers both geometric properties and spatial relationships between points, improving classification accuracy in complex environments. Recent updates have enhanced Cyclone 3DR's ability to handle large-scale datasets through optimized memory management and parallel processing capabilities.

Figure 17. Result of Cyclone 3DR Automatic Point Cloud Classification

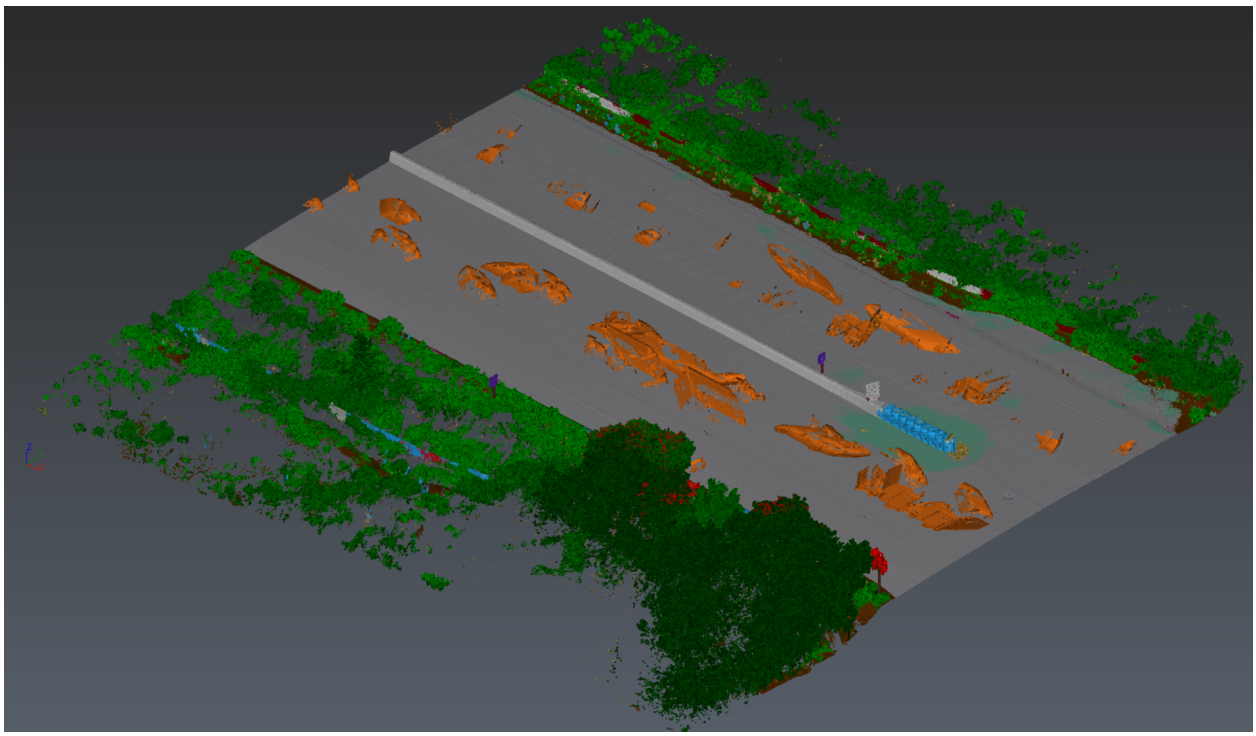

Result of Cyclone 3DR automatic point cloud classification.

Table 4. Comparative Analysis of LiDAR Processing Software

Feature	**TBC**	**GMP**	**Cyclone 3DR**
Ground Classification	Accurate	Accurate	Accurate
Power Line Classification	Weak	Superior	Good
Lane Marking Extraction	Robust for roads	Not applicable	Works well
Ease of Use	Moderate (manual corrections)	High (automated workflow)	Moderate (some training needed)
Customization	High (detailed settings)	Moderate	High (rule-based)
AI/Deep Learning	ML-assisted	No AI models	Limited AI customization
Performance on Noisy Data	Struggles with noise	Handles well	May misclassify noisy data

- **Lane Markings**: TBC outperforms other platforms in lane marking and curb feature extraction, offering superior accuracy in detecting pavement markings and roadway boundaries.

- **Power Lines**: GMP excels in power line and pole classification, leveraging specialized algorithms for high-accuracy overhead conductor detection, making it ideal for utility corridor mapping.

- **Customization vs. Automation**: TBC provides greater customization for advanced users, while GMP's automated workflow prioritizes efficiency and ease of use, catering to standard applications.

- **Misclassification Challenges**: Both tools struggle with poles and complex structures, particularly in overlapping or intricate geometries, emphasizing the need for algorithm improvements in future updates.

TBC, GMP, and Cyclone 3DR each excel in different aspects of LiDAR point cloud processing. TBC is best for lane marking and road feature extraction, while GMP outperforms in power line classification, making it ideal for utility mapping. Cyclone 3DR offers AI-assisted versatility but may require fine-tuning in noisy datasets.

TBC provides greater customization, benefiting advanced users, whereas GMP's automated workflow enhances efficiency. Both tools face misclassification challenges, highlighting the need for algorithm improvements. The choice of software depends on project needs, with future advancements in AI and automation crucial for enhancing classification accuracy.

3.4 Deep Learning Point Classification Using Python

Deep learning has emerged as a powerful approach for classifying LiDAR point clouds due to its ability to learn complex patterns and features directly from raw data. Unlike traditional rule-based classification methods, deep learning models can automatically extract features, enabling more accurate and efficient classification of ground, vegetation, buildings, and other objects in LiDAR datasets. This section explores the application of deep learning techniques for point cloud classification using Python-based frameworks.

Overview of Deep Learning Models for Point Cloud Classification

Deep learning models, including Convolutional Neural Networks (CNNs), Recurrent Neural Networks (RNNs), and, more recently, PointNet and PointNet++ architectures have been widely adopted for point cloud processing. These models offer several advantages, including the ability to automatically extract spatial features without manual input, the scalability to handle large-scale

point clouds efficiently, and the capability to achieve higher classification accuracy compared to traditional methods.

Data Preparation for Deep Learning

Effective deep learning-based point cloud classification requires comprehensive data preprocessing, including normalization to ensure uniform scale and distribution of point coordinates, segmentation to divide the point cloud into smaller, manageable sections for focused analysis, and feature engineering to incorporate additional features such as intensity, RGB values, normal vectors, curvature, height above ground, and point density to improve model accuracy

Training and Evaluation

The training process for deep learning models involves several key components. A loss function, such as cross-entropy loss, is used for multi-class classification tasks to measure the difference between predicted and actual outcomes. An optimizer, such as the Adam optimizer with a learning rate scheduler, is employed to enhance convergence and efficiently update model parameters during training. The batch size, which refers to the number of data samples processed together in one iteration, is set based on memory constraints and dataset size, typically ranging from 16 to 64 points per batch.

Evaluation metrics are crucial for assessing the performance of a trained model. Accuracy, defined as the percentage of correctly classified points, provides an overall measure of how well the model performs. Precision and recall are used to evaluate the model's ability to correctly identify each class, offering insights into the model's performance on individual categories. Intersection over Union (IoU) is another important metric that assesses the overlap between predicted and actual classes, which is particularly useful in evaluating segmentation tasks.

3.4.1 Deep Learning Point Classification Test

Experiment Setup

- Programming Environment: Python 3.8 with TensorFlow 2.10, CUDA 11.8, and cuDNN 8.6.
- Libraries Used: NumPy for data handling, TensorFlow for model implementation, Open3D for point cloud processing, and Scikit-learn for evaluation metrics.
- Hardware Configuration: Windows 11 Desktop NVIDIA GeForce RTX4090 Graphic card GPU with CUDA support for accelerated training.

Preprocessing

Label data (or classification) was created using with Trimble Business Center for Tile 1-30. The total number of points is 500,324,404.

Figure 18. Labeled Data for Deep Learning Point Cloud Classification

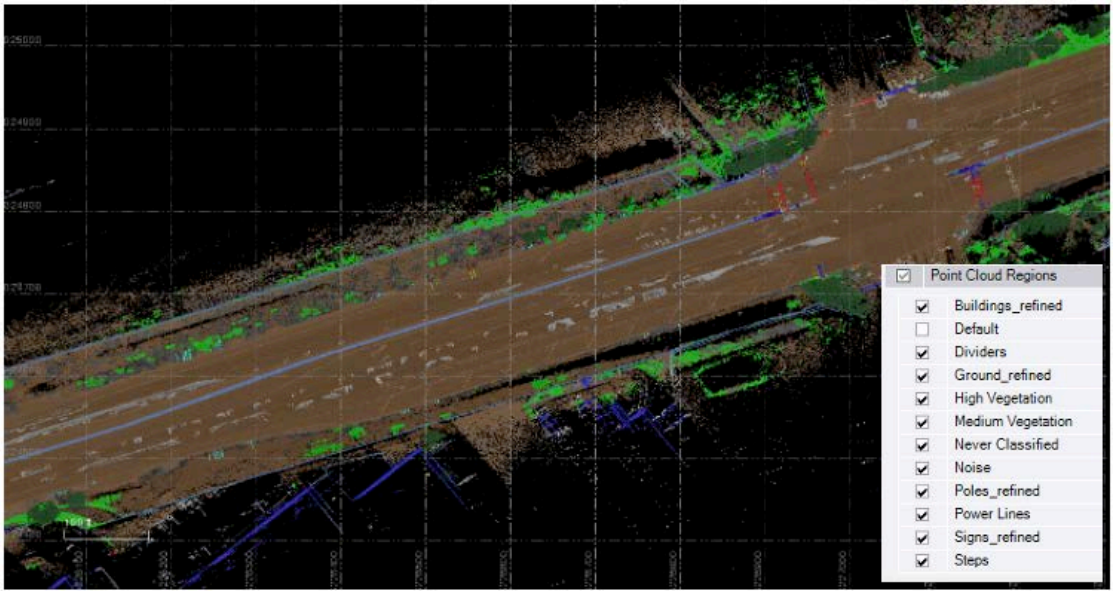

Table 5. Labeled Data Statistics

Class	# of points	Percentage	Description
Class 0	312,859	0.06	Never Classified
Class 1	6,117,425	1.22	Unclassified
Class 2	407,113,080	81.37	Ground
Class 4	35,509,503	7.10	Medium Vegetation
Class 5	23,144,068	4.63	High Vegetation
Class 6	24,181	0.00	Building
Class 7	3,895,234	0.78	Noise
Class 14	33,331	0.01	Power Lines
Class 65	970,398	0.19	Poles
Class 66	416,120	0.08	Signs
Class 79	22,788,205	4.55	Dividers
Total	500,324,404	100.00	

Table 5 show the point statistics of labeled data. Class 2 (ground) takes 81%; the next classes—Class 4 and 5—are vegetation which take 7.1% and 4.6%, respectively, and together 11.7%. Class 79, Dividers, takes 4.6%.

To efficiently handle and train on large-scale point cloud data, a preprocessing script was implemented to divide the full dataset into manageable chunks. The script loads seven precomputed features—XYZ coordinates, intensity, surface normals, curvature, density, height above ground (HAG), and classification labels—from .pkl files and splits them into 25-million-point segments. Each segment is saved individually using consistent naming conventions, enabling efficient disk-based streaming during model training without overloading the memory.

Multi-Layer Perception Training

A PointNet-style multi-layer perceptron (MLP) model was trained for binary classification of ground versus non-ground points using chunked LiDAR point cloud features. Seven features—XYZ coordinates, intensity, and normals—were extracted and standardized using a streaming StandardScaler. To address class imbalance, binary labels were created by remapping selected classes, and class weights were computed. The model was trained on 25-million-point chunks using PyTorch with GPU acceleration, reduced memory usage via float16 tensors, and batch-wise data loading. The training process saved both the model and the feature scaler for later inference.

Classification (or Inferencing)

To classify new point cloud data, we developed an inference pipeline that loads a raw LAS file and extracts essential features including XYZ coordinates, intensity, surface normals, curvature, point density, and height above ground (HAG). The features are computed using Open3D and NumPy. The processed data is then scaled using a previously trained StandardScaler and passed through a pretrained PointNet-based binary classifier implemented in PyTorch. The model infers ground (class 1) versus non-ground (class 0) points in batches for memory efficiency. The resulting classifications are written back into the original LAS structure and saved as a new classified LAS file.

Classified LAS Result

First, binary classification for ground and non-ground and multi-class classification were performed.

Figure 19. Python-based Point Cloud Classification Result

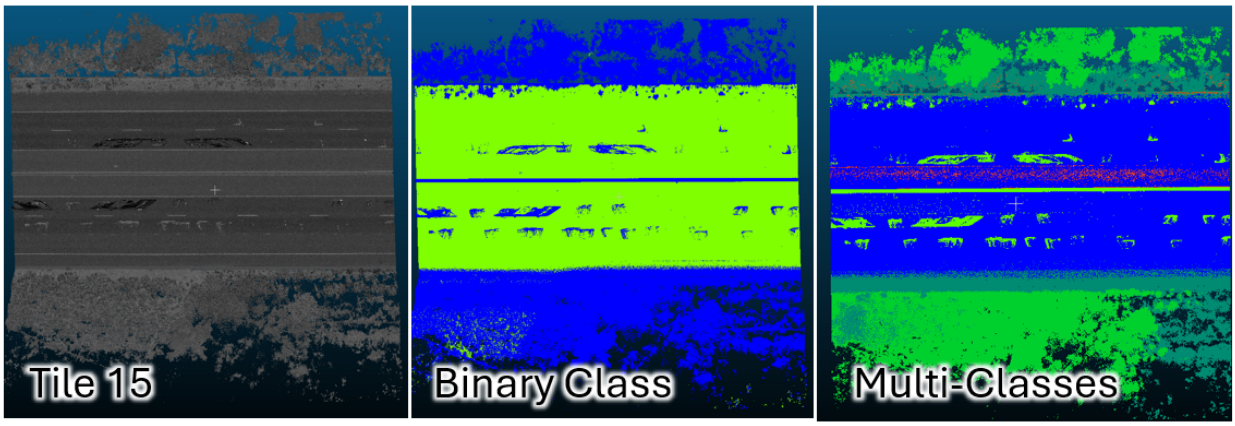

Original point cloud (left), binary classification (middle), and multi-class classification (right).

Figure 20. Point Cloud Classification Result for Tile 14, 15, and 16

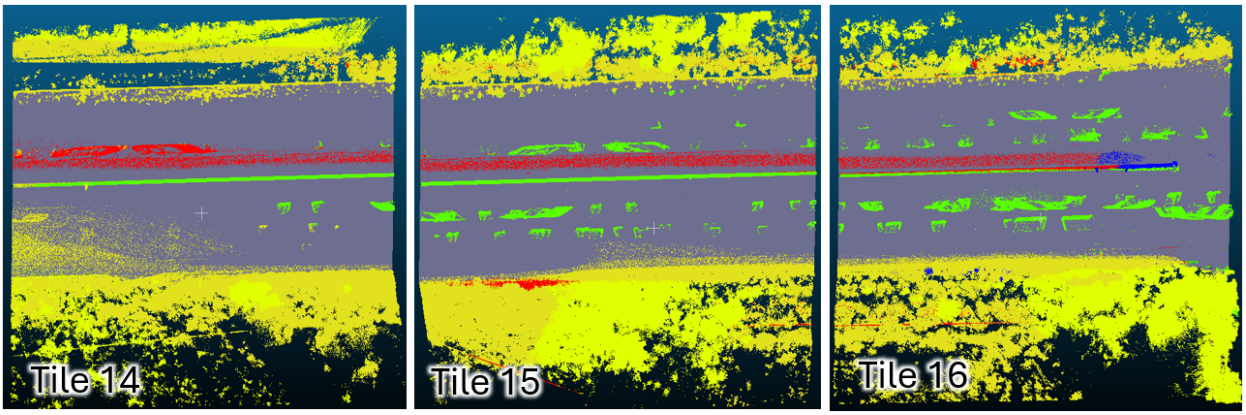

The results in Figures 19 and 20 demonstrate the effectiveness of the Python-based point cloud classification pipeline. As shown in Figure 19, the original point cloud (left) was first processed for binary classification (middle), distinguishing ground from non-ground points. Subsequently, a more detailed multi-class classification (right) was applied, accurately identifying distinct classes such as road surfaces, vehicles, vegetation, and building structures. Figure 20 further illustrates the model's performance across three tiles (14, 15, and 16), where consistent and structured class boundaries are evident, especially along road features and surrounding environments. These results indicate that the deep learning-based classifier, trained on mobile LiDAR data, can generalize well across neighboring tiles and handle high-density point clouds with complex scenes.

Summary and Conclusion

This study demonstrates a complete end-to-end workflow for extracting and classifying roadside assets from high-density mobile LiDAR point cloud data. The approach integrates traditional geospatial techniques—such as raster generation and slope profiling—with modern deep learning-based point classification using a customized PointNet model.

Over 5.7 billion points were processed, and more than 500 million labeled points were used to train the classifier. Results show high accuracy in both binary ground/non-ground and multi-class classification scenarios. Figures 19 and 20 illustrate the classifier's effectiveness across various tiles, successfully distinguishing roads, curbs, vegetation, poles, and other urban features.

The modular and scalable design of this pipeline enables its application to large datasets and diverse roadway environments. Compared to existing commercial software, the deep learning approach offers improved automation and generalizability, while maintaining interpretability and control.

In conclusion, this project confirms that deep learning can significantly enhance the automation, scalability, and accuracy of mobile LiDAR data processing. Future directions include extending the model to support more fine-grained classification (e.g., lane markings, traffic lights) and deploying the workflow in near-real-time mapping or autonomous driving applications.

Glossary

AI – Artificial Intelligence

AASHTO – American Association of State Highway and Transportation Officials

CNN – Convolutional Neural Network

DEM – Digital Elevation Model

GNSS – Global Navigation Satellite System

HAG – Height Above Ground

IMU – Inertial Measurement Unit

LAS – LASer File Format

LAZ – Compressed LAS

LiDAR – Light Detection and Ranging

MLP – Multi-Layer Perceptron

MTLS – Mobile Terrestrial Laser Scanning:

PCD – Point Cloud Data

TBC – Trimble Business Center

TIN – Triangulated Irregular Network

Bibliography

Cao, J., Song, C., Song, S., Xiao, F., & Peng, S. (2019). Lane detection algorithm for intelligent vehicles in complex road conditions and dynamic environments. *Sensors*, *19*(14), 3166.

Gargoum, S., & El-Basyouny, K. (2017, August). Automated extraction of road features using LiDAR data: A review of LiDAR applications in transportation. In *2017 4th International Conference on Transportation Information and Safety (ICTIS)* (pp. 563–574). IEEE.

Gargoum, S. A., & El Basyouny, K. (2019). A literature synthesis of LiDAR applications in transportation: Feature extraction and geometric assessments of highways. *GIScience & Remote Sensing*, *56*(6), 864–893.

Garzón Barrero, J., Cubides Burbano, C. E., & Jiménez-Cleves, G. (2021). Quantifying the effect of LiDAR data density on DEM quality. *Ciencia e Ingeniería Neogranadina*, *31*(2), 149–169.

Hu, Y. (2003). Automated extraction of digital terrain models, roads and buildings using airborne LiDAR data (pp. 85–88). University of Calgary, Department of Geomatics Engineering.

Javeed, M. A., Ghaffar, M. A., Ashraf, M. A., Zubair, N., Metwally, A. S. M., Tag-Eldin, E. M., ... & Jiang, X. (2023). Lane line detection and object scene segmentation using otsu thresholding and the fast hough transform for intelligent vehicles in complex road conditions. *Electronics*, *12*(5), 1079.

Kim, H., Arrowsmith, J., Crosby, C. J., Jaeger-Frank, E., Nandigam, V., Memon, A., ... & Baru, C. (2006, December). An efficient implementation of a local binning algorithm for digital elevation model generation of LiDAR/ALSM dataset. In *AGU Fall Meeting Abstracts* (Vol. 2006, pp. G53C-0921).

Kumar, P., McElhinney, C. P., Lewis, P., & McCarthy, T. (2013). An automated algorithm for extracting road edges from terrestrial mobile LiDAR data. *ISPRS Journal of Photogrammetry and Remote Sensing*, 85, 44–55.

Lin, Y. C., Liu, J., Cheng, Y. T., Hasheminasab, S. M., Wells, T., Bullock, D., & Habib, A. (2021). Processing strategy and comparative performance of different mobile lidar system grades for bridge monitoring: A case study. *Sensors*, *21*(22), 7550.

Liu, X., Zhang, Z., Peterson, J., & Chandra, S. (2007). LiDAR-derived high quality ground control information and DEM for image orthorectification. *GeoInformatica*, *11*, 37–53.

Pfeifer, N., Dorninger, P., Haring, A., & Fan, H. (2007). Investigating terrestrial laser scanning intensity data: quality and functional relations.

Pingel, T. J., Clarke, K. C., & McBride, W. A. (2013). An improved simple morphological filter for the terrain classification of airborne LIDAR data. *ISPRS Journal of Photogrammetry and Remote Sensing*, 77, 21–30.

Rashdi, R., Garrido, I., Balado, J., Del Río-Barral, P., Rodríguez-Somoza, J. L., & Martínez-Sánchez, J. (2024). Comparative evaluation of LiDAR systems for transport infrastructure: Case studies and performance analysis. *European Journal of Remote Sensing*, *57*(1), 2316304.

Sithole, G., & Vosselman, G. (2004). Experimental comparison of filter algorithms for bare-Earth extraction from airborne laser scanning point clouds. *ISPRS Journal of Photogrammetry and Remote Sensing*, *59*(1–2), 85–101.

Soilán, M., Riveiro, B., Martínez-Sánchez, J., & Arias, P. (2017). Segmentation and classification of road markings using MLS data. *ISPRS Journal of Photogrammetry and Remote Sensing*, *123*, 94–103.

Williams, K., Olsen, M. J., Roe, G. V., & Glennie, C. (2013). Synthesis of transportation applications of mobile LiDAR. *Remote Sensing*, *5*(9), 4652–4692.

Yu, Y., Li, J., Guan, H., Jia, F., & Wang, C. (2014). Learning hierarchical features for automated extraction of road markings from 3-D mobile LiDAR point clouds. *IEEE Journal of Selected Topics in Applied Earth Observations and Remote Sensing*, *8*(2), 709–726.

Yang, R., Li, Q., Tan, J., Li, S., & Chen, X. (2020). Accurate road marking detection from noisy point clouds acquired by low-cost mobile LiDAR systems. *ISPRS International Journal of Geo-Information*, *9*(10), 608.

About the Authors

Yushin Ahn

Yushin Ahn is an Associate Professor of the Department of Civil and Geomatics Engineering, California State University (CSU) at Fresno, CA. He received a B. Eng. Degree in civil engineering and an M.Sc. degree in surveying and digital photogrammetry from Inha University, Korea in 1998 and 2000, and an M.sc. and PhD degree in geodetic science from the Ohio State University, Columbus, in 2005 and 2008 respectively. His research interests include digital photogrammetry, feature tracking, and sensor calibration and integration. Dr. Ahn received the Robert E. Altenhofen Memorial Scholarship from American Society of Photogrammetry and Remote Sensing. He has been a certified photogrammetrist since 2014.

Riadh Munjy

Dr. Riadh Munjy received his BS in Civil Engineering in 1978 from the University of Baghdad, Iraq, an MSCE in civil Engineering in 1979, an MS in Applied Mathematics in 1981, and a PhD in Civil Engineering in 1982 from the University of Washington. He has been a faculty member and an active researcher at CSU, Fresno since 1982 and has been a Professor of Civil and Geomatics Engineering since 1988 and the Chair of the Civil and Geomatics Engineering Department since 2014. He has over forty years of experience in teaching courses in photogrammetry, digital mapping, GIS, and least squares adjustment. He was awarded the Meritorious Service Award by ASPRS in 1997, the Fairchild Photogrammetric Award in 2014, the Fellow Award in 2020, and the Lifetime Achievement Award in 2023.

Steven Choi

Dr. Stephen Choi is an Associate Professor of Information Systems at CSU, Fresno. He received his PhD in Information Systems from the College of Computing Sciences, New Jersey Institute of Technology. His research interests focus on the Artificial Intelligence domain where machine learning, deep learning, and reinforcement learning with business data are emphasized. Dr. Choi stays active with AI education where he is the AI certificate program coordinator and is involved with AI course development and pedagogies. Before joining college academics, Dr. Choi worked as a business professional and manager for over ten years with leading companies such as Pfizer Pharmaceuticals, Johnson & Johnson Pharmaceuticals, and Covance.

MTI FOUNDER

Hon. Norman Y. Mineta

MTI BOARD OF TRUSTEES

Directors